Universidade de Aveiro
2008

Departamento de Engenharia Mecânica

Raquel Maria Amaro Vaz

Crescimento e Caracterização de Filmes de Diamante em Substratos de Aço

Growing and Characterisation of Diamond Coatings on Steel Substrates

Universidade de Aveiro
2008

Departamento de Engenharia Mecânica

Raquel Maria Amaro Vaz

Crescimento e Caracterização de Filmes de Diamante em Substratos de Aço

Growing and Characterisation of Diamond Coatings on Steel Substrates

Dissertação apresentada à Universidade de Aveiro para cumprimento dos requisitos necessários à obtenção do grau de Mestre em Engenharia Mecânica, realizada sob a orientação científica do Doutor José Joaquim de Almeida Grácio, Professor Catedrático do Departamento de Engenharia Mecânica da Universidade de Aveiro

Apoio financeiro da FCT, no âmbito
do Programa POCI/EME/60816/2004

o júri

presidente

Prof. Dr. Francisco José Malheiro Queirós de Melo
professor associado do Departamento de Engenharia Mecânica da Universidade de Aveiro

Prof. Dr. José Joaquim de Almeida Grácio (orientador)
professor catedrático do Departamento de Engenharia Mecânica da Universidade de Aveiro

Prof. Dr. Orlando Manuel Neves Duarte Teodoro
professor associado do Departamento de Engenharia Física da Universidade Nova de Lisboa

agradecimentos

Expresso aqui os meus sinceros agradecimentos a todos aqueles que directa ou indirectamente contribuíram para a concretização deste trabalho, sem que me permita deixar de referir algumas pessoas em particular.

Ao caríssimo Professor Doutor Grácio por todo o apoio dado na orientação deste trabalho e pelo optimismo que sempre me incutiu.

Ao Victor Neto, pela sua ajuda e disponibilidade constantes e pela camaradagem nos momentos mais cruciais.

À Professora Mónica Oliveira pela sua receptividade e espírito crítico.

Agradeço toda a amabilidade e apoio na análise de amostras, especialmente ao Professor Jorge Soares, do Departamento de Física e à Marta Ferro, do Departamento de Engenharia Cerâmica e do Vidro.

Um especial agradecimento, a todos a quem incomodei com as minhas questões, e que foram muitos, o que me impede de enumerá-los.

A todos os novos amigos que tive oportunidade de fazer e aqueles mais antigos, o meu muito obrigada por tudo.

Por último, embora em lugar cimeiro, agradeço aos meus mais queridos a compreensão pelas minhas ausências.

palavras-chave

Diamante; CVD com modulação temporal; aço; morfologia; propriedades mecânicas

resumo

Os revestimentos de diamante têm um grande potencial em diversas aplicações tecnológicas, devido às suas excelentes propriedades, permitindo uma melhoria no desempenho de componentes mecânicos e o aumento do seu tempo de vida útil. Os aços possuem um interesse especial, dada a sua viabilidade no fabrico de uma vasta gama de componentes de engenharia. Ainda assim, para aplicações de maior exigência, a deposição por via química em fase de vapor (CVD) de um revestimento de diamante aderente sobre o aço, poderá trazer grandes vantagens.

A indústria em geral, e particularmente, o sector da produção de moldes para injecção de plásticos, tem vindo a investir rumo a novas soluções no sentido de aumentar a resistência ao atrito e desgaste dos moldes. Os revestimentos de diamante CVD poderão aumentar a vida dos moldes e melhorar potencialmente a qualidade das peças produzidas, diminuindo a percentagem de não conformidades. Contudo, a implementação deste processo de revestimento a nível industrial ainda não foi possível, dadas, entre outras, as dificuldades que estão associadas à deposição de diamante em substratos de aço.

Esta dissertação relata um estudo sobre o crescimento de filmes de diamante em substratos de aço. Os substratos testados consistiram em amostras de aço AISI P20 modificado, um material vulgarmente utilizado em moldes de injecção de plásticos. Foram também investigados, e em termos comparativos, os aços: AISI 304, 310 e 316. Os filmes de diamante foram depositados por meio de uma técnica recentemente desenvolvida de CVD com modulação temporal, por isso designado, como *time-modulated* CVD (TMCVD). Em todas as amostras, foi utilizada uma camada intermédia de nitreto de crómio (CrN).

Foram investigados vários ciclos de deposição a fim de encontrar o melhor compromisso entre qualidade e o crescimento de filmes contínuos. A deposição de filmes de diamante em substratos de aço AISI P20 modificado e AISI 304 foi bem sucedida. Foi realizada a caracterização morfológica dos filmes depositados. Foram também avaliadas, a dureza, as tensões residuais e a adesão dos filmes. O aço AISI P20 modificado revestido com diamante, através da técnica de deposição TMCVD, mostrou ter enorme potencial, para aplicações tecnológicas.

keywords Diamond; time-modulated CVD; steel; morphology; mechanical properties

abstract

Diamond coatings have an exceptional potential for different technical applications because of its extraordinary properties, allowing the improvement of mechanical components performance and increasing tools life time. Steel have a special interest because of its general use on the manufacture of a wide range of engineering components with good suitability. Although, for more demanding applications, the deposition on steel of a well adherent diamond coating by chemical vapour deposition (CVD) could have great advantages.

The industry, particularly the plastics injection moulding industry, is investing in new solutions in order to improve friction and wear behaviour of the moulds. Diamond CVD coatings could be a good contribution to the increase of moulds life time, potentially improving the quality of injected parts and reducing non-conformities. However, the industrial implementation of such a coating process could not be realized yet, since diamond coating of steel comes along with several technical problems.

This dissertation reports a study on diamond growing on steel substrates. The substrate materials tested were made from AISI P20 modified steel, commonly used in the manufacturing of moulds for the plastic injection moulding industry. Also, and for comparison, samples of AISI 304, 310 and 316 were tested. Diamond films were deposited using a recently developed method called time-modulated CVD (TMCVD). In all the samples a chromium nitride (CrN) intermediate layer was used.

Different deposition cycles were investigated in order to achieve the best compromise between film quality and film growth rate. Diamond films were successfully deposited onto AISI P20 modified and AISI 304 steels. A morphological characterisation of films was performed. Hardness, residual stresses and adhesion were evaluated. Diamond deposition on AISI P20 modified steel substrates using TMCVD show promising results for technological applications.

Contents

List of Tables

List of Figures

Motivation and Outline

The deposition of diamond films by chemical vapour methods brought new possibilities to take advantage of the unique properties of diamond for several applications. The use of chemical vapour deposition (CVD) diamond coatings in the industry could be the key to improve components performance and life time. Diamond coating of steel parts have a great potential for technological applications, due to the large percentage those materials represent in mechanical and tools industry.

Mechanical components and metal tools face everyday more demanding performance requirements and the use of surface coatings creates the possibility for a material design in which specific properties are located where they are required. Particularly, plastic injection moulding industry is making big efforts in finding new surface treatments to improve friction and wear behaviours, among other properties. Diamond CVD coatings could be a good contribution to the improvement of tools for the plastics industry, increasing moulds life time and potentially improving the quality of injected parts and reducing non-conform products. Toward the industrial implementation of such a process, it is necessary to find ways to solve a series of questions, since diamond coating of steels faces several difficulties.

A big delay in the application of those coatings on steel substrates is associated to the difficulty in obtaining well adherent films. This fact is a global result from different substrate/film system contributions. Differences in physical behaviours beneath deposition conditions and principally, through the final stage of cooling, are crucial to determine the effectiveness of coating adhesion to the substrate. The high difference between thermal expansion coefficients of substrate and diamond coating is a source of compressive stresses in the coating after the cooling process, leading to a lack of adhesion and causing eventual delamination or film cracking.

The present dissertation reports a study made on CVD diamond coating on different steel substrates. Diamond coatings were deposited using an innovative method, based on methane (CH_4) flow rate modulations, named time-modulated CVD (TMCVD). The novelty in this work consists in the experiments to deposit CVD diamond films on austenitic stainless steels using TMCVD processes.

Different TMCVD cycles were tested to achieve the growth of continuous and good quality diamond films on the substrates. A chromium nitride (CrN) interlayer was

deposited on the substrate surface in order to improve diamond film adhesion. The films were morphologically characterised. Residual stresses, hardness and adhesion were also evaluated.

The outline of this dissertation consists in four chapters. Chapter 1 provides a general review of the state of the art on diamond deposition and the last developments on the subject. It is included a summary of the available deposition techniques, namely hot filament CVD (HFCVD) that was the used process. Also, it is presented a complete description of the main features of TMCVD process.

In chapter 2, a description of characterisation techniques and experimental methods commonly used in coated systems is presented, focusing on the employed methods: scanning electron microscopy (SEM), Raman spectroscopy and hardness tests.

Chapter 3 show the main results obtained in terms of morphology and nucleation rates of diamond films, in correlation with the TMCVD deposition parameters of each experimental cycle. Nucleation densities, growing rates and films morphology were analysed by SEM. Besides preliminary experiments on AISI 316 and 310 steel samples, continuous TMCVD diamond films were grown on two different steel substrates: AISI P20 modified (W. Nr. 1.2738) and AISI 304, a typical injection mould steel and an austenitic stainless steel, respectively.

The adhesion of the films was estimated by indentation testing. Residual stresses were measured through the shifting of the films Raman spectra, from diamond characteristic line. A comparative study of residual stresses in the different coatings was also performed. The variation of composite hardness of the substrate/interlayer/diamond film systems was evaluated by hardness and micro-hardness measurements.

In chapter 4, it is presented a summary of the main conclusions obtained from the present research. Additionally some suggestions for future work are given.

Chapter 1.

State of the Art

1.1 Properties of Diamond

Different forms of carbon, the six most abundant element in the universe [1], are being exploited in terms of innovative engineering applications. Graphite and diamond are the better known forms of elemental carbon found in nature. The difference between them is the way that carbon atoms are arranged. Diamond is essentially a regular tetrahedral arrangement of carbon atoms with sp^3 hybrid bonding [2]. The diamond crystal can be defined as two interpenetrating face-centered cubic (fcc) lattices, as illustrated in figure 1.1.

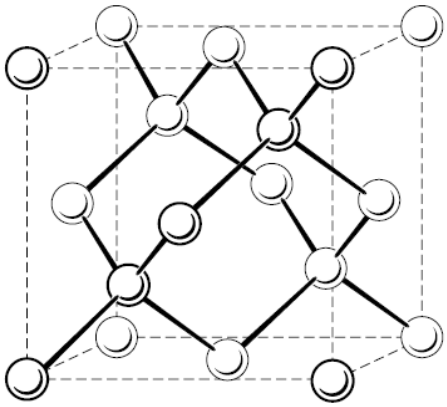

Figure 1.1. Illustration of diamond crystal lattice structure [3].

In diamond lattice structure, each carbon atom is tetrahedrally coordinated, forming strong covalent bonds with its four neighbours using hybrid sp^3 atomic orbitals and creating a totally covalent crystalline structure. In graphite lattice structure, each carbon atom is covalent bonded to three neighbour atoms using hybrid sp^2 atomic orbitals and forming a series of continuous hexagonal structures located in parallel planes linked by van der Waals bonds, much weaker than covalent bonds [3]. To illustrate these features, figure 1.2 presents the lattice structures of graphite and diamond.

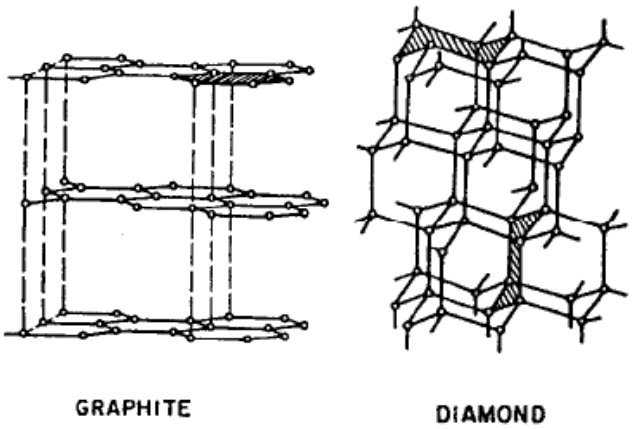

Figure 1.2. Illustrations of graphite and diamond lattice structures [4].

As carbon atoms in diamond are strength covalent bonded, it is required a significant energy to remove a carbon atom from the diamond lattice. This feature justifies the high hardness and abrasion resistance of diamond whereas graphite is soft and lubricating.

Diamond can also exist in a series of polytypes, as: cubic, 3C-hexagonal and 2H-hexagonal diamond, also known as loansdaleite. The other crystalline forms of carbon besides diamond and graphite, are carbyne in sp^1 hybridization and fullerenes in a combination of sp^2 and sp^3 hybridization [2].

Diamond is a unique engineering material since its extraordinary combination of physical, chemical and mechanical properties. A selection of some of these properties of diamond is presented in table 1.1. A more detailed list of properties and related effects can be found at reference [4].

Table 1.1. Some notable properties of diamond [5]

Extreme mechanical hardness	~100 GPa
High thermal conductivity	$2x10^3$ W/m.K (at room temperature)
Low thermal expansion coefficient	$0.8x10^{-6}$ K^{-1} (at room temperature)
High bulk modulus	1200 GPa
Chemical inertness and corrosion resistance	

To understand diamond nucleation and growth processes during chemical vapour deposition (CVD), the knowledge of atomic and crystal structures of diamond is essential, as well as the competing crystallites or amorphous phases that may occur by CVD.

Carbon has an outer electronic configuration $2s^2$ $2p^2$ and can hybridize forming triangle sp^2 or tetrahedral sp^3 bonds. Three hybrid carbon orbitals available for bonding: sp, sp^2, and sp^3, complete the series of electronic building blocks of all carbon allotropes and compounds. Besides other species, the most significant competition during CVD process occurs between sp^2 and sp^3 types of carbon, i.e., graphite and diamond structures.

Recent evolutions on the techniques for diamond films deposition are making possible to take advantage of the excellent properties of diamond opening the way for new applications. Table 1.2 present some of the main properties of CVD diamond and possible applications.

Table 1.2. Properties of CVD diamond and some applications [2, 4]

Property	CVD Diamond	Possible applications
Vickers hardness (kg/mm^2)	12000-15000	Drills, polishing materials, cutting tools
Coefficient of friction (in air)	0.1	Wear resistance coatings on lenses, bearings, tools or hard disks, sliding parts
Young's modulus (N/m^2)	$1.2x10^{12}$	Micromechanical applications
Chemical inertness	inert	Coatings for reactor vessels, sample container for analytical instruments
Thermal conductivity (room temperature) ($W\ cm^{-1}\ K^{-1}$)	20	Insulating heat sinks for high power electronic compounds

CVD diamond was rapidly developed in the last years as a method to produce films for a diversity of industrial applications, as in optical, thermal, mechanical and electronics. The properties of CVD diamond are almost the same that of natural diamond; however, there are a few problems to solve yet. The adhesion of diamond to non-diamond substrates for tribological applications and the impurities on diamond coatings for optical and electronic applications need to be improved. Efforts in that sense are been done, as it will be presented in this chapter.

1.2 Deposition Techniques

Even with its extreme physical properties, natural diamond use in science or engineering has been restricted, since its scarcity and high cost. Efforts to synthesize diamond artificially were made using graphite as a starting material, which demonstrates to be very difficult due to this form of carbon being the thermodynamically stable allotrope at room temperature and pressure [6].

The knowledge of the conditions under which natural diamond is formed suggested that diamond could be formed by heating carbon under extreme pressure [6]. Based on that principle, a high-pressure high-temperature (HPHT) method was successfully developed by General Electrics in 1959. Applying pressures in the range of 50-100 kBar and temperatures around 1800-2300 K, HPHT was used to produce synthetic diamond crystals during decades [7 and ref. within]. But it was still necessary an evolution to more economical techniques which could originate diamond in more functional forms, as thin films.

Since initial discovery of diamond CVD films in the 1950s by Eversole and its confirmation by Angus and his team, in the late 1960s [5], diamond films found extensive applications in industry. Because of the difficulty in depositing superior diamond films being nearly as extreme as its unique properties [8], a wide range of film-coating technologies have been investigated in order to deposit diamond on a variety of substrate materials. Diamond thin films produced via CVD represent a largely used technology, with enormous potential for several commercial applications [9], although the limitation of substrate materials imposed by the relatively high deposition temperatures around 700-900 ºC [1, 6]. CVD diamond deposition demonstrates to be the most successful method, due to the high degree of sp^3 bonding of the resulting films [6].

In the next sections; after a brief consideration on CVD process and principles, it will be explained the working principle of HFCVD, being this the diamond deposition method selected for the experiments presented on this study.

1.2.1 Chemical Vapour Deposition (CVD)

A basic principle to grow diamond on a substrate is the existence in the region adjacent to the substrate material, of a gas-phase in a non-equilibrium condition, created by a gas-phase activation process [10]. Depending on the activation sources for chemical reactions, these processes could be achieved by thermal activation, laser-assistance or plasma-assistance [4,6,7,11]. The activation of the gas phase carbon-containing precursor molecules, can involve thermal methods, as in hot-filament; plasma, direct current (DC), radio frequency (RF) or microwave, or a combustion flame, such as an oxyacetylene torch [4,7]. The features that distinguish the reactors are the deposition area, growth rate, quality, uniformity and reproducibility. All the methods have common requirements to growth high quality diamond films

CVD involves a gas phase chemical reaction above a material surface, originating deposition onto that surface. Methane (CH_4) is the mainly carbon-containing gas used to synthesize diamond by CVD. In addition to a carbon carrier, the deposition atmosphere should normally contain efficient non-diamond carbon compounds etchants, being hydrogen (H_2) the most common gas applied on this propose. The precursor gas is added in excess of H_2 [7]. In an atmosphere with methane and hydrogen, the percentage of hydrogen must reach around 97 to 99 vol. % in the mixture to allow the growth of diamond films with high quality [4].

Some of the roles for atomic hydrogen in diamond nucleation include the generation of specific gas-phase species that promote nucleation and growth of diamond; hydrogenation of unsaturated carbon bonds on the surface to promote sp^3 bonding, preferential etching of non-diamond carbon species and stabilization of the diamond surface [12].

(A) Fundamentals

CVD is a process where one or more gaseous adsorption species react or decompose on a hot surface to form stable solid products. More complex than physical vapour deposition (PVD) techniques, CVD exhibits the advantages of producing highly pure and dense films at reasonably deposition rates [10]. The method allows coating uniformly complex shape components, due to its non-line-of-sight nature.

PVD involves the generation of vapour phase species either via evaporation, sputtering, laser ablation or ion beam [10]. The main characteristics of those techniques that distinguish them from CVD methods is that the start material or the material to deposit, already exists in the solid state and it is converted in vapour by heating (evaporation) or collisions with charged particles (ions, electrons, photons) [13].

Surface mechanisms occurring during deposition can lead to the growth of both diamond and graphite phases, depending namely on the operating conditions. Besides others, are included various gas precursors molecules as CH_3, C_2H_2, CH and C atoms.

Surface reactions usually starts with the abstraction of a surface hydrogen (H) atom by a gas-phase H atom, creating a reactive radical on the surface that can be efficiently terminated by another gas-phase H atom. This last reaction is easier than the initial H abstraction. Those reactions of H abstraction and H termination are quicker reactions in relation to the other processes occurring during deposition. The relation of the rates of H abstraction and H termination reactions determinates the fraction of reactive radicals on the deposition surface. CH_x(x = 0-3) radicals compete with atomic H for the open radicals, even if the hydrocarbon adsorption is much slower [4].

Some determinant factors can influence the crystallite size. Those factors are: gas composition; flow rate and pressure, substrate temperature, substrate surface pre-treatment and film thickness. By changing the growth conditions, diamond films can be deposited with properties ranging from almost graphitic to essentially characteristic of natural diamond.

As an example, the growth rate increases as the CH_4 concentration is increased [14], promoting a crystal size decrease due to the enhancement of nucleation density and the appearance of secondary nucleation on the firstly existing diamond crystal facets [4]. In the presence of high CH_4 concentrations, amorphous carbon or diamond-like carbon species can be formed [5].

Previous studies demonstrate that diamond growth rate increases with power and gas pressure [5,14,15]. The effect of power is mainly an effect of substrate temperature. Higher CH_4 concentrations and gas pressure result in higher nucleation density and growth rate but with lower film quality. It was found that gas flow rate has small influence on the diamond nucleation density and growth rate [14,16].

The effect of substrate temperature on diamond nucleation and growth has also been investigated [17]. According to the results on previews works, it is possible to prove that substrate temperature is a key parameter in CVD diamond nucleation, growth and film quality. For constant deposition parameters, lower substrate temperature origins reduced nucleation and inferior film quality. The rate of secondary nucleation is expected to increase with deposition temperature [18].

Usually, to grow diamond rather than other forms of carbon, the substrate temperature must be superior to 700 ºC [6]. This condition promotes a preferential growth of diamond relatively to graphite. Those factors will be considered in more detail on the section of the diamond growing mechanisms.

A substrate pre-treatment is the better way to decrease the initial delay in nucleation previous to individual crystallites appearance, so called incubation period. A role of methods for surface pre-treatment has been studied to promote the nucleation density and film adhesion. Those methods include scratching of substrate surface with abrasive powders, polishing with diamond pastes or powders with different particle sizes, seeding with diamond crystals, substrate negative d.c.-biasing or bias-enhanced nucleation (BEN) and ultrasonic treatments [2,4].

Diamond residues remaining on the substrates surfaces after polishing and abrasion with diamond powders are believed to provide nucleation sites, enhancing nucleation density [9]. Higher nucleation densities can be obtained with diamond powders of smaller particle sizes, particularly below 3 μm. Also, it was found that the nucleation density increases proportionally to the polishing time [19, 14].

Negatively biasing the substrate has been suggested to increase the flux of carbon-containing cations and accelerate these reactive species towards the substrate. Ion bombardment results in higher energy being transferred to the surface and hence increases the surface mobility of adsorbed species [21].

Studies on copper substrates demonstrate that BEN effectively enhances diamond nucleation on these substrates [21]. Charged particles formed in the plasma bombard the substrate and create nucleation sites on the surface. A negative potential, usually 100 to 200 V [6], is applied to the substrate heater during the initial minutes of the process. This would accelerate the carbon-containing ions onto the substrate, promoting the creation of a carbon-rich layer in the substrate top-superficial layers, contributing both to the increase of

initial nucleation rates and to the growth of films with a preferred orientation. Details concerning those and other methods can be found on the references [2,4,21].
In the aim of this work, the samples were pre-treated by ultrasonic seeding in a 1/4 μm diamond powder suspension.

1.2.1.1 Hot Filament Chemical Vapour Deposition (HFCVD)

In 1982, Matsumoto and his group built a hot filament reactor at the National Institute for Research in Inorganic Materials (NIRIM) obtaining promising results [6 and ref. within].
HFCVD is perhaps the simplest method to growth diamond at low pressures. The process involves a gas mixture containing CH_4 and H_2, normally with volume percentage in H_2 much higher than in CH_4 , in the order of 0.1 to 2 vol.% of CH_4 in H_2 [4].
The gases are introduced in a vacuum chamber, and flow through the filament, usually made of tungsten (W) or tantalum (Ta), that is electrically heated to temperatures around 2000-2400 ºC [4]. The substrate is mounted at a distance of a few millimetres from the filament and heated to the deposition temperature. The filament metal is supposed to resist to those temperatures without melting and to have a reduced reactivity with the gas phases, although Ta and W carburize and form metal carbide under diamond deposition conditions with effects on its performance and duration.
Despite these typical conditions, each deposition parameter must be regulated and the overall deposition conditions should be selected according to film requirements and applications. Quality and properties of a diamond film, can be easily tailored to suit particular applications.

Even with a good reproducibility, HFCVD has several limitations associated to the filament in what concerns to stability and life-time, and films contamination by metal evaporation from it. The formation of carbides during the incubation and deposition stages, affect the filament stability [4].
Comparatively to the other methods, HFCVD have advantages in terms of simplicity and associated costs, offering some unique advantages in terms of scalability for the deposition of diamond over large areas [22]. Growth rates for polycrystalline diamond HFCVD films can be in the range of 1-10 μm h^{-1} [6]. Generally, higher growing rates correspond to a loss

of film quality. Here, quality refers to an evaluation of the ratio of sp^3 to sp^2 bonding, as well as C-C against C-H bonding content and crystallinity [7].

(A) Fundamentals

A complex role of chemical reactions and physical processes occur during the deposition process. After introducing the gases, they mix and diffuse to the substrate surface. When the precursor gases molecules pass through the filament, they receive thermal activation energy and dissociate into reactive radicals and atoms, which continue to chemically react until they reach the substrate surface. At this point, they can adsorb and react with the surface; desorb back to the gas phase, or diffuse around close to the surface until an appropriate reaction site is found [6]. When a surface reaction takes place and if the conditions are appropriated, a diamond film could be formed. This complex set process is schematically represented in figure 1.3.

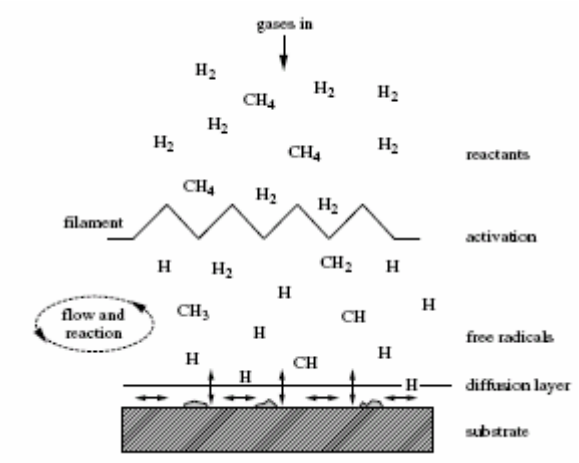

Figure 1.3. HFCVD reactions sequence [6].

One important reaction product from the gas phase dissociation is atomic hydrogen. In this deposition method, atomic hydrogen is formed via thermal decomposition of H_2 when passing through the heated filament. Atomic hydrogen concentration act as a critical element for several processes occurring during diamond deposition, namely: (a) stabilising the sp^3 diamond lattice, so preventing surface graphitisation, (b) etching sp^2 graphitic carbon during diamond growth, (c) reacting with CH_4 and creating radicals that are able to link to appropriate surface sites.

1.3 Time-modulated Chemical Vapour Deposition (TMCVD)

A significant limitation for a wide scale use of diamond coatings is the high roughness of the as-grown CVD films [21]. Conventional CVD techniques provide polycrystalline diamond films presenting columnar growth characteristics mainly responsible for the high surface roughness of the films. Additionally, during deposition, intrinsic stresses are induced into the growing films due to the non-uniform growth profile of the films, which degrades their properties [24].

There are a diversity of methods to control the films surface roughness and morphology. The most common include post-deposition treatments, such as mechanical or chemical mechanical polishing, induction on the deposition conditions as nitrogen doping, nucleation methods, as bias-enhanced nucleation and nanoparticles seeding, besides others [21,17].

In order to control microstructure and roughness of diamond films, Fan et al. [24] developed a new process assigned time-modulated chemical vapour deposition (TMCVD), being the first paper on the subject published in 2002 [24]. For comparison, the process was implemented for diamond deposition using a HFCVD and a microwave CVD systems [21, 27]. TMCVD allows depositing smoother polycrystalline diamond films at relatively higher growth rates in comparison with conventional CVD techniques.

The fundamental difference between the two methods is that in traditional CVD, all the deposition conditions are kept constant during the deposition process, whereas TMCVD involves pulsing CH_4 gas. CH_4 is pulsed into the vacuum reactor alternating between high and low flow rates for predetermined periods of time, during whole diamond CVD cycle. The initial diamond nucleation stage occurs at higher CH_4 concentration, followed by a lower CH_4 concentration during the growth period. Those fluctuations are repeated a number of times during the deposition process, what justifies the process name: ‘time-modulated’ CVD.

Ali et al. [28] found that the increase of CH_4 concentration promotes effectively the overall nucleation density, although deteriorating the quality of the films in terms of diamond carbon phase purity. Long growth periods under high methane concentrations leads to the incorporation of non-diamond carbon phases in the films, such as graphite and amorphous

[24]. When the CH_4 flow rate is reduced, diamond crystals grow in columnar way as in traditional CVD processes. Increasing again the CH_4 concentration will result in a promoted secondary nucleation of diamond grains on top of the already existing crystals, where the surface energy is lower, fulfilling surface irregularities.

In the lower pulses of CH_4 flow rate, the higher H_2 concentration enhances the non-diamond phases etching. This feature justifies the fact that TMCVD process ends with a low CH_4 flow rate. Figure 1.4 means to illustrate the growing mechanisms of TMCVD in comparison with a conventional CVD process using a HFCVD system.

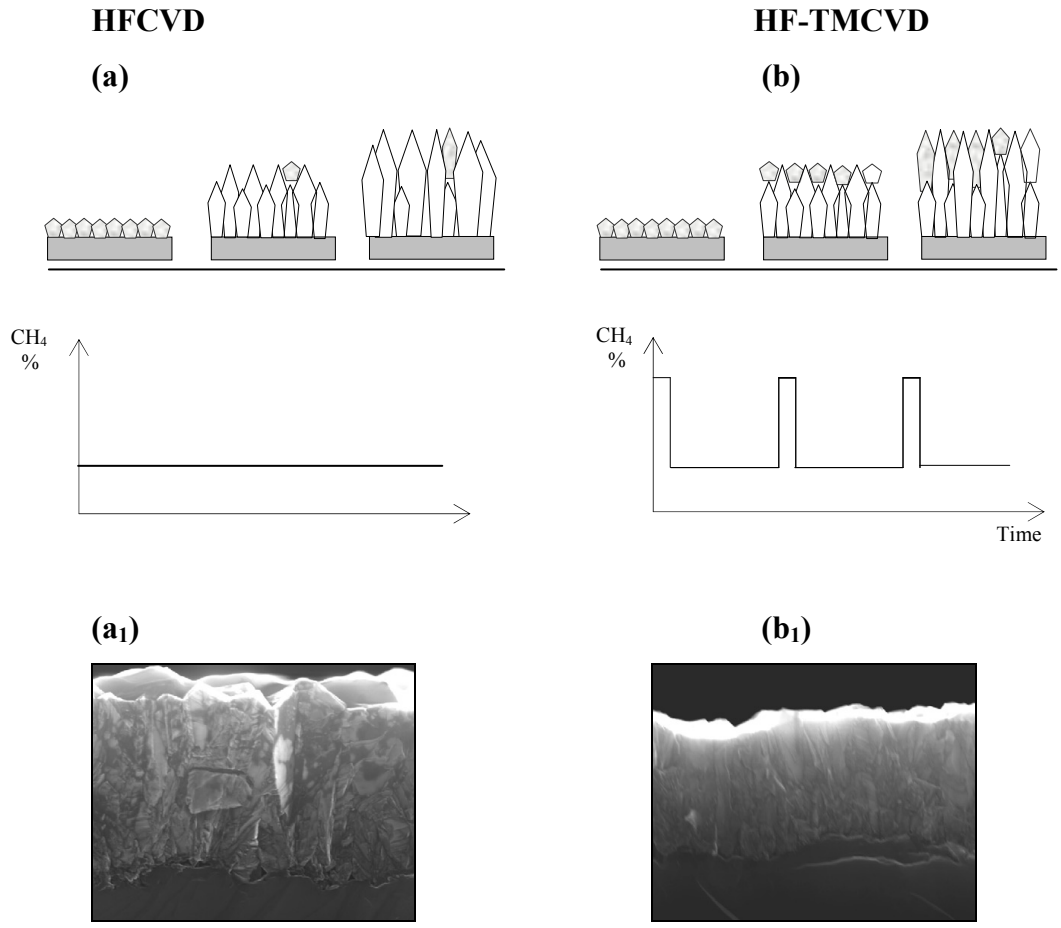

Figure 1.4. Comparison of preliminary mechanisms of film growth during conventional HFCVD and HF-TMCVD processes (a, b) and SEM images showing the surface profiles of grown films (a_1, b_1) [9].

The deposition process effectively results in the formation of multilayered diamond coatings involving nucleation stage, diamond growth and secondary nucleation, cyclically repeated [21]. In comparison with conventional CVD methods, TMCVD present numerous advantages [18-19]:

- reduced processing times
- relatively improved growth rates
- quicker initial diamond nucleation
- improved secondary nucleation
- improved film coverage
- better coating adhesion

Analogous film quality was obtained when comparing with conventional CVD films; but improved graphite etching during growing stages at low CH_4 and high H_2 levels. Also, smoother films were achieved for the same thickness, than in conventional CVD films, formed by smaller diamond crystallites, were the growing is inhibited by secondary nucleation during CH_4 peaks (micro- and nanocrystalline diamond coatings) [19]. The TMCVD process enables to control the film morphology; crystals present columnar growth as in conventional CVD, but smaller crystals can be obtained with TMCVD.
The optimisation of the TMCVD process can effectively diminish processing times and resources investment, being the main advantage of the method and making it well suitable for industrial production purposes [18,20,21].

1.4 CVD Diamond Growing Mechanisms

To describe a crystal lattice, it is normally used an x, y, z coordinate system associated to the different crystal faces. The three most important surfaces for diamond adsorption and growth are the square (100) surface, the triangular (111) surface, and a less well-defined (110) surface [6].

The kinetics for diamond growth on each different surface possesses growth rates depending differently on temperature and gas phase composition. This kinetics can be used to control the morphology of the obtained crystals.
According to Wild et al. [29], an assigned α-parameter is frequently used to determine the shape of single crystals, given by the following relation:

$$\alpha = \sqrt{3}\frac{\upsilon_{100}}{\upsilon_{111}} \tag{1.1}$$

where υ_{100} and υ_{111} represent the growth velocities in the (100) and (111) directions, respectively. The morphology of the crystals is characterized by the ratio of the (100) to the (111) growth rates. Single crystals present $\alpha = 1$ for cubes, $\alpha = 3$ for octahedra and $1 < \alpha < 3$ for cubo-octahedra [6], as illustrated in figure 1.5.

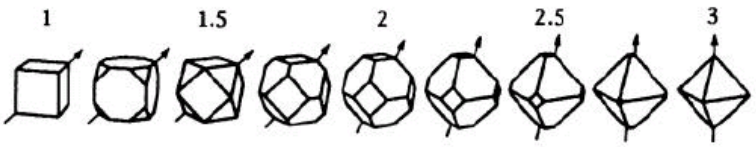

Figure 1.5. Idiomorphic crystal shapes for different values of the growth parameter, α; the arrows indicate the direction of fastest growth [4].

In the case of polycrystalline films, α-parameter controls the films structure and morphology [29, 30]. CVD diamond film surface morphology depends critically on the process parameters, especially the gas mixing ratio. This ratio determines the value for the α-parameter. In CH_4/H_2 systems, depending on the ratio of the two gases, the film can be randomly oriented, (111) triangular preferentially orientated, or (100) square faceted.

CVD diamond films deposited onto non-diamond substrates exhibit generally a similar polycrystalline morphology, of randomly oriented crystals in the presence of non-diamond carbon and defects [4]. This polycrystalline morphology can vary from well-defined facets to very irregular forms. For low deposition temperatures and low CH_4 concentrations, octahedral crystals with {111} faceting are predominant [31]. With a continuous increasing in the deposition temperature and/or carbon concentration, there is a morphological

evolution to cubo-octahedra composed of both {111} and {100} facets; later to cubic {100} facets and for superior super-saturation conditions, to a spherical shape morphology [33].

The surface morphology is very sensitive to the gas phase mixing ratio and it is also affected by the substrate temperature. In figure 1.6 is shown how the film morphology is affected, either by deposition temperature and methane/hydrogen ratio for CVD.
Under low CH_4 partial pressure and low substrate temperature, triangular {111} facets tend to be dominant; at relatively superior concentrations of CH_4 in the gas mixture, and/or for higher substrate temperatures, {100} square and rectangular facets begin to prevail.

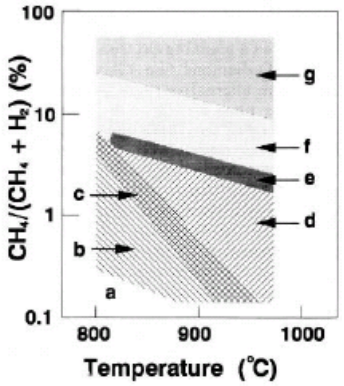

Regions:

a) little or no deposition of either diamond or graphite
b) {111} faces predomination
c) {111} and {l00} faces with similar frequency
d) {100} faces predomination
e) {100} faces predominate and diamond grains grow preferentially along <100> axis
f) films with a smooth surface composed by diamond nanocrystals and disordered graphite
g) films surface composed of fibrous deposits of soot or disordered graphite growing vertically from the surface

Figure 1.6. Representative diagram of film morphology as a function of deposition temperature and CH_4/H_2 ratio for CVD between 30-80 Torr [7].

Diamond growth begins when carbon atoms nucleate in a surface in an appropriate way to initiate the beginnings of a sp^3 tetrahedral lattice. In natural diamond substrates the growth is homoepitaxial, the template for the required tetrahedral structure is already there, and the diamond lattice is simply extended atom by atom.
In non-diamond substrates, diamond growth is heteroepitaxial. C atoms that deposit in such surfaces are immediately etched back into the gas phase by reaction with atomic H [6]. As a result, the initial induction period before which diamond starts to grow can be prohibitively long. For that reason, substrate surfaces often suffer a pre-treatment prior to deposition in order to reduce induction times for nucleation and to increase the nucleation sites density, as discussed in the previous section.

After individual diamond crystallites had nucleated on the surface, the growing occurs in three dimensions until crystals coalescence to form a continuous film. The growing film is polycrystalline, presenting numerous grain boundaries and defects and exhibiting a columnar structure extending upward from the substrate. As the film thickness increases, the crystals become bigger while the number of defects and grain boundaries decreases. This feature justifies the fact that external layers of thicker films have usually much better quality than the initial nucleating layers.

Some investigations reveal that increasing methane concentrations, crystal sizes decreases until 3% CH_4/H_2, where the crystalline morphology disappears [34]. Such a film, is sometimes named as nanocrystalline or 'ballas' diamond, and can be considered to be an aggregate of diamond nanocrystals and disordered graphite. Those films are much smoother than polycrystalline films.

1.5 CVD Diamond on Steel Substrates

Hard coatings represent an important market segment in the world economy [2]. Generally, it is fundamental to adjust the coating properties to a specific application. In the case of mechanical proposes a special attention should be given to the control of hardness, surface roughness and film adhesion. However, the ability of the coating to protect the substrate, enhancing the mechanical and tribological properties of the composite system relies essentially on the deposition process, morphology, elemental composition and microstructure [35].

Diamond coating on steel surfaces presents some difficulties and although some evolutions presented on this field, those films are difficult to deposit directly on steel [36].

Nucleation has a crucial dependence on the chemical nature and surface condition of the substrate [21]. The growth of diamond from the vapour phase depends highly on the nature of the non-diamond substrates and can be divided into three main categories: (a) strong carbide forming materials, as Si, Ti, Cr, W, SiC and WC, (b) strong carbon dissolving, as Fe, Co, Ni and (c) small or no affinity to carbon materials, as Cu and Au [38].

Carbide-forming substrates are normally suitable for diamond deposition. Non-carbide forming substrates are also used to grow diamond for many applications, but requiring a

previous surface pre-treatment or the use of an intermediate layer. Among these variety of substrates, Si is the most commonly used substrate in CVD diamond synthesis due to its nature of carbide formation and similarity in the lattice structure with diamond. Also, a well-known and strongly adherent system is obtained with diamond growing on molybdenum (Mo) substrates [41].

The formation of graphite during CVD is problematic, especially in the cases when the substrate material contains iron (Fe), nickel (Ni) and cobalt (Co) [8,39, 40].

Fe works as a catalyst for graphite formation on the substrate surface during diamond deposition [17], growing a thick graphite layer on the surface. Diamond growth on this layer is possible but with a serious lack of adhesion, enabling technical applications of the resulting films. Another difficulty on depositing diamond on steel substrates has a great contribution from the large diffusion of carbon into the steel at CVD temperatures, leading to a very low diamond nucleation and degradation of steel properties. The high solubility of carbon in the austenite, a face centred cubic (fcc) phase of Fe [46], the formation of cementite (Fe_3C) iron carbide in this phase [42] and the formation of graphite, alter negatively the steel properties. Also, the large difference in thermal expansion coefficients promotes the creation of compressive stresses in the interface between steel and diamond originating the film delamination.

Considering mechanical and tribological applications of coated parts, the effect of intrinsic and extrinsic stresses on the adherence between diamond films and substrate materials is very important. The adhesion of diamond films on steel substrates was found to be relatively weak, mainly because of the residual stresses created in the film. In order to improve the adhesion, numerous attempts have been done. One of the most common solutions is the use of interlayers between the steel substrate and the diamond deposited film, as gradient interlayers, multiple interlayer systems or single layers.

Although efforts made to improve deposition results via a number of surface pre-treatment methods [6,9,21], the use of interlayers is the most generalised solution to diamond deposition effectiveness and adhesion improvement.

Those interlayers or multilayer systems should be able to meet some requirements: (i) act as a diffusion barrier against both the diffusion of carbon from the gas phase to the substrate and iron from the bulk substrate to the surface; (ii) present good adhesion either to diamond coating and substrate, (iii) possess intermediate mechanical and physical

properties among substrate and diamond film, in order to promote a gradient transition between film and substrate material.

Particularly, the employment of an interlayer with an intermediate thermal expansion coefficient between substrate and film is an excellent approach, leading to a decrease of the interfacial stress effects, avoiding either carbon diffusion into the substrate and formation of sp^2 carbon at the interface during the deposition process [42].

For those proposals, a large number of different interlayers had been applied successfully on steel substrates, namely, SiC [43], TiN [44] boride modified surface layers [41], TiC [52, 42], Ni/Cu/Ti [47], TiC/Ti(C,N)/TiN [42], TiBN [46], and many others.

The use of chromium carbide diffusion interlayers resulting from chromizing processes demonstrate to produce well adherent CVD diamond coatings on steel [50,51]. Several works of successfully CVD diamond deposited on steel substrates using chromium nitride (CrN) interlayers, prepared either by physical vapour deposition or nitridation of electroplated Cr coatings, have been reported in the last years [41,53,54].

CrN has a thermal expansion coefficient (α_{CrN} = 7.14 x10^{-6} K^{-1} [32]) similar to diamond ($\alpha_{diamond}$ = 0.8x10^{-6} K^{-1} [52]), from which its application as an interlayer is expected to develop low residual thermal stress in the diamond film, improving diamond films adhesion on the samples. Although the apparent success of this solution, residual stresses could still result large enough to originate a film delamination.

Nitrided chromium and diffusion chromized interlayers were described as successful in the accommodation of high thermal stresses present on ferritic tool steels, presenting an improved diamond film adhesion. Nevertheless, in the case of austenitic stainless steels the adhesion of deposited diamond films remains poor, due to the relatively higher thermal expansion coefficient. Borges et al. [54] employed a nitriding process to increase the amount of CrN on AISI 304 stainless steel samples surface, obtaining high nucleation density and a uniform diamond film with good adhesion.

In the recent years, a number of investigations have been performed in diamond coatings on steels substrates, with positive results, as presented in the references [36,46,47,56], for example. The present research work means to collaborate in this evolution.

References

1. J. Filik, “Raman Spectroscopy: a simple, non-destructive way to characterise diamond and diamond-like materials”, SpectroscopyEurope, Volume 17 5 (2005)
2. H.S. Nalwa, Handbook of Thin Film Materials, Volume 2: Characterization and spectroscopy of thin films, Chapter 3, (2002) 115- 147
3. B.S. Mitchell, An introduction to materials engineering and science: for chemical and materials engineers, John Wiley & Sons, Inc. Publication, chapter 1 (2004) 59
4. H. Liu, D. S. Dandy, Diamond chemical vapour deposition - nucleation and early growth stages, Noyes Publications, chapters 2,3 (1995) 8-13, 14-45
5. Q.H. Fan, “Diamond deposition on metals”, University of Aveiro-Portugal, PhD Thesis (1998)
6. P.W. May, “Diamond thin films: a 21st-century material”, Philosophical Translations of the Royal Society of London A, 358 (2000) 473-495
7. M.N.R. Ashfold, P.W. May, C.A. Rego and N.M. Everitt, “Thin film diamond by chemical vapour deposition methods”, Chemical Society Reviews, (1994) 21-30
8. W. Zhu, P.C. Yang, J.T. Glass, F. Arezzo, “Diamond nucleation and growth on reactive transition-metal substrates”, Journal of Materials Research 10 (1995) 1455
9. N. Ali, Q.H. Fan, T. Huang. V.F. Neto, Y. Kousar, W. Ahmed and J. Grácio, “Time-modulated CVD process for producing smoother diamond coatings”, New Developments on Tribology: Theoretical Analysis and Application to Industrial Processes – University of Aveiro, (2002) 121
10. S.C. Tjong and Haydn Chen, “Nanocrystalline materials and coatings”, Materials Science and Engineering R 45 (2004) 1- 88
11. H.O. Pierson, Handbook of Chemical Vapour Deposition – principles, technology and applications, 2nd edition, Noyes Publications, chapter 2 (1999) 36-58
12. A. Elshabini and F.D. Barlow, Thin Film Technology Handbook, Charles A. Harper, Series Advisor, McGraw-Hill, chapter 7 (1998) 1-63
13. J.M. Albella, “*Láminas delgadas y recubrimientos, preparación, propiedades y aplicaciones*”, *Consejo Superior de Investigaciones Científicas CSIC(II)* (2002) 27-35

14. Q.H. Fan, E. Pereira and J. Grácio, "Diamond deposition on copper: studies on nucleation, growth, and adhesion behaviours", Journal of Materials Science 34 (1999) 1353 – 1365
15. D. Das, V. Jayaseelan, R. Ramamurti, R.S. Kukreja et al., "Low surface temperature synthesis and characterization of diamond thin films", Diamond and Related Materials 15 (2006) 1336-1349
16. T. Chunjiu, "*Hidrogénio em filmes de diamante crescidos por CVD assistido por plasma*", University of Aveiro-Portugal, PhD Thesis (2004)
17. M.J. Jackson, G.M. Robinson, W. Ahmed, H. Sein, A.N. Jones, N. Ali, E. Titus, Q.H. Fan and J. Grácio, "Time-modulated Chemical Vapour Deposition of Diamond Films", Journal of Materials Engineering and Performance 14 (2005) 163- 172
18. N. Ali, V.F. Neto, Sen Mei, G. Cabral, Y. Kousar, E. Titus, A.A. Ogwu, D.S. Misra and J. Grácio, "Optimisation of the new time-modulated CVD process using the Taguchi method", Thin Solid Films 469–470 (2004) 154–160
19. N. Ali, G. Cabral, A.B. Lopes and J. Grácio, "Time-modulated CVD on 0.8 μm-WC–10%-Co hardmetals: study on diamond nucleation and coating adhesion", Diamond and Related Materials 13 (2004) 495–502
20. V.F. Neto, "Investigation of the film properties of advanced diamond coatings deposited using time-modulated CVD", MSc dissertation, University of Aveiro, (2004)
21. N. Ali, Q.H. Fan, W. Ahmed, I.U. Hassan, C.A. Rego and I.P. O' Hare, "Role of surface pre-treatment in the CVD of diamond films on copper", Thin Solid Films, 355-356 (1999) 162-166
22. J.W. Zimmer, G. Chandler and T. Sharda, "Wide area polycrystalline diamond coating and stress control by sp^3 hot filament CVD reactor", Thin Solid Films 516 (2008) 696-699
23. N. Ali, Q.H. Fan, Y. Kousar, W. Ahmed and J. Grácio, "Implementation of the time-modulated process to produce diamond films using microwave-plasma and hot-filament CVD systems", Vacuum 71 (2003) 445 – 450
24. N. Ali, Q.H. Fan, T. Huang. V.F. Neto, Y. Kousar, W. Ahmed and J. Grácio, "Time-modulated CVD process for producing smoother diamond coatings", New

Developments on Tribology: Theoretical Analysis and Application to Industrial Processes – University of Aveiro, (2002) 121

25. S. Takeuchi, S. Oda, M. Murakawa, "Synthesis of multilayer diamond film and evaluation of its mechanical properties", Thin Solid Films 398-399 (2001) 238-243
26. Q.H. Fan, N. Ali, W. Ahmed, Y. Kousar, and J. Grácio, "Novel time-modulated chemical vapor deposition process for growing diamond films", Journal of Materials Research, 17 7, (2002) 1563
27. N. Ali, V.F. Neto, and J. Grácio, "Promoting secondary nucleation using methane modulations during diamond chemical vapor deposition to produce smoother, harder, and better quality films", Journal of Materials Research, 18 (2) (2003) 296
28. N. Ali, Q.H. Fan, W. Ahmed and J. Grácio, "Deposition of polycrystalline diamond films using conventional and time modulated CVD processes", Thin Solid Films 420 - 421 (2002) 155 – 160
29. C. Wild, P. Koidl, , W. Müller-Sebert, H. Walcher et al., "Chemical vapour deposition and characterization of smooth{100}faceted diamond films", Diamond and Related Materials 2 2-4 (1993) 158-168
30. C. Wild, R. Kohl, N. Herres et al., "Oriented CVD diamond films: twin formation, structure and morphology", Diamond and Related Materials 3 4-6 (1994) 373-381
31. J.C. Angus, and C.C. Hayman, "Low-pressure, metastable growth of diamond and 'diamond-like' phases", *Science,* 241 (4868) (1988) 913-921
32. G.C.A.M. Janssen, F.D. Tichelaar, C.C.G. Visser, "Stress gradients in CrN coatings", Journal of Applied Physics 100, 093512 (2006)
33. K. Kobashi, K. Nishimura, Y. Kawate, and T. Horiuchi, "Synthesis of diamonds by use of microwave plasma CVD: morphology and growth of diamond films", Physical *Review B,* 38 (1988) 4067
34. A. Gicquel, K. Hassouni, F. Silva and J. Achard, "CVD diamond films: from growth to applications", Current Applied Physics 1 (2001) 479-496
35. N.J.M. Carvalho, "Low friction and wear resistant coatings –microstructure and mechanical properties", PhD Thesis, Groningen University Press- Netherlands, (2001)
36. J.G. Buijnsters, P. Shankar and J.J. Ter Meulen, "Direct deposition of polycrystalline diamond onto steel substrates", Surface & Coatings Technology 201 (2007) 8955-8960
37. See f. ex. webpage *www.prirev.pt* (11.11.2007)

38. N. Ali, G. Cabral, E. Titus, A.A. Ogwu and J. Grácio, "Characterization of diamond adhesion on micro-grain WC-Co substrates using Brinell indentations and micro-Raman spectroscopy", Journal of Physics: Condensed Matter 16 (2004) 6661-6674
39. H.-G. Jentsch, G. Rosenbauer, S.M. Rosiwal, R.F. Singer, "Graphite interlayer formation during CVD diamond coating of iron base alloys: the analogy to metal dusting", Advanced Engineering Materials 2 6 (2000) 369–374
40. X. Chen, J. Narayan, "Effect of the chemical nature of transition-metal substrates on CVD of diamond", Journal of Applied Physics 74 (1993) 4168
41. J.G. Buijnsters, P. Shankar, W.J.P. van Enckevort, J.J. Schermer and J.J. ter Meulen, "The adhesion of hot-filament CVD diamond films on AISI type 316 austenitic stainless steel", Diamond and Related Materials 13 (2004) 848-857
42. R. Polini, F.P. Mantini, M. Braic et al., "Effects of Ti- and Zr-based interlayer coatings on the hot filament chemical vapour deposition of diamond on high speed steel", Thin Solid Films 494 (2006) 116-122
43. I. Endler, A. Leonhardt, H.-J. Scheibe and R. Born, "Interlayers for diamond deposition on tool materials", Diamond and Related Materials 5 (1996) 299-303
44. P.S. Weiser and S. Prawer, " Chemical vapour deposition of diamond onto iron based substrates – the use of barrier layers", Diamond and Related Materials 4 (1995) 710-713
45. Q.H. Fan, A. Fernandes, E. Pereira and J. Grácio, "Adhesion of diamond coatings on steel and copper with a titanium interlayer", Diamond and Related Materials 8 (1999) 1549-1554
46. J.C. Bareiβ, G. Hackl, N. Popovska, S.M. Rosiwal, R.F. Singer, "CVD diamond coating of steel on a CVD-TiBN interlayer", Surface & Coatings Technology 201 (2006) 718–723
47. F.J.G. Silva, A.J.S. Fernandes, F.M. Costa, A.P.M. Baptista et al., "A new interlayer approach for CVD Diamond coating of steel substrates, Diamond and Related Materials 13 (2004) 828-833
48. M. Ohring, Materials Science of Thin Films- deposition and structure, 2nd edition, chapter 10 (2001) 559-640
49. Z.L. Wang, "Transmission electron microscopy of shape-controlled nanocrystals and their assemblies", Journal of Physics and Chemistry B, 104, (2000) 1153-1175

50. S. Schwarz, Y. Musayev, S.M. Rosiwal, C. Schaufler, R.F. Singer and H. Meerkamm, “High temperature diffusion chromizing as a successful method for CVD-diamond coating of steel”, Diamond and Related Materials 11 (2002) 757–762
51. S. Schwarz, S.M. Rosiwal, Y. Musayev and R.F. Singer, “High temperature diffusion chromizing as a successful method for CVD-diamond coating of steel - part II”, Diamond and Related Materials 12 (2003) 701–706
52. R. Polini, G. Mattei, R. Valle and F. Casadei, “Raman spectroscopy characterization of diamond films on steel substrates with titanium carbide arc-plated interlayer”, Thin Solid Films 515 (2006) 1011-1016
53. A. Fayer, O. Glozman, and A. Hoffman, “Deposition of continuous and well adhering diamond films on steel”, Applied Physics. Letters 67 16 (1995) 2299-2301
54. C.F.M. Borges, E. Pfender, J. Heberlein, “Influence of nitrided and carbonitrided interlayers on enhanced nucleation of diamond on stainless steel 304”, Diamond and Related Materials 10 (2001) 1983-1990
55. M. Ohring, The Materials Science of Thin Films, Academic Press, Inc., chapter 14 (1992) 635
56. C. Bareiβ, M. Perle, S.M. Rosiwal, R.F. Singer, “Diamond coating of steel at high temperatures in hot filament chemical vapour deposition (HFCVD) employing chromium interlayers”, Diamond & Related Materials 15 (2006) 754–760

Chapter 2.

Experimental Methods and Characterization Techniques

In the current research work, a set of steel samples were diamond coated on a hot-filament chemical vapour deposition (HFCVD) system. A brief description of the equipment and system procedures is presented on the first section of this chapter.
The fundamentals of the characterization techniques employed to analyse the deposited samples, are introduced in the subsequent sections of the chapter. Characterization techniques include: scanning electron microscopy (SEM), Raman spectroscopy and hardness testing.
For the evaluation of residual stresses, a method based on the Raman diamond line shifting was used. For the estimation of the films adhesion, a method based on the behaviour of the coated samples under distinct indentation loads, was employed. Those experimental methods will also be described on this chapter.

2.1 HFCVD Reactor and Experimental Procedures

A HFCVD reactor (Criolab, Portugal) [1], available in the research unit TEMA (Centre for Mechanical Technology and Automation) in the Department of Mechanical Engineering of the University of Aveiro, was used for diamond deposition.
Figure 2.1, shows a picture of the HFCVD equipment. The system consists in a power source and related components, a reactor chamber with around 5x5 cm usable area for the samples, an automated gas distribution system, a vacuum pump system and a computerized process control and data acquisition, to control the gas inlet and monitor the filament temperature.

Figure 2.1. HFCVD reactor used for diamond films production [2].

A schematic representation of the system components can be seen in figure 2.2. As discussed in chapter 1, the main process parameters in the deposition system are gas pressure, gas phases flow rates and filament power. Those values can be read directly from the system, and optimized for different purposes. Table 2.1 summarise the range of deposition parameters possible to obtain in the HFCVD reactor.

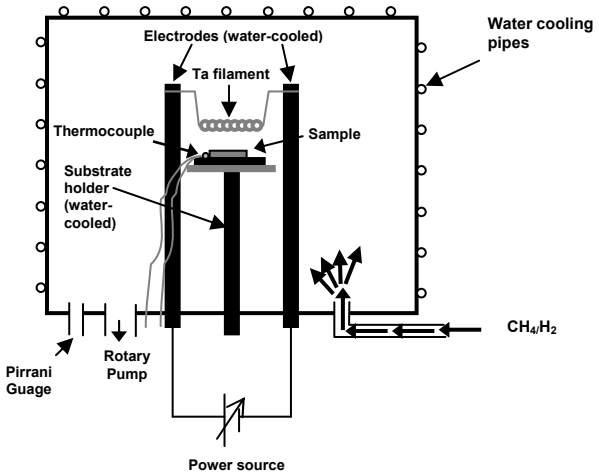

Figure 2.2. Experimental setup HFCVD system used for diamond films production (adapted from [1]).

The filament consists in a tantalum wire. Usually, before the deposition process, the filament is carburised to minimize tantalum contamination of the coating [20]. During

deposition, the filament is maintained at a temperature around 2100-2300 ºC, in order to activate the process gases, CH_4 and H_2.

The substrate temperature is measured using a K-type thermocouple, mounted directly facing the substrate during the deposition. The filament temperature is measured by an IMPAC optical pyrometer.

Table 2.1. TMCVD range of deposition parameters

Parameter	Value
Pressure	10^{-3}- 10^{3} Torr
H_2 flow rate	0 - 400 sccm
CH_4 flow rate	0 - 10 sccm
Current	0 - 30 A
Voltage	0 - 45 V

The synthesis of diamond with the HFCVD system comprises basically the following steps:

(a) Substrate sample preparation. The samples are cut to the desired dimension and suffer a polishing treatment. Usually, in the case of steel samples, this step consists in a mechanical abrasion with a sequence of SiC sand papers, followed by diamond powder or pastes, until a mirror finishing is obtained. The samples are cleaned with an alcohol or acetone and dried.

(b) HFCVD ramp up. After placing the substrate into the reactor chamber, the system is ready to be started to diamond deposition. The system deposition procedures sequence is summarised in figure 2.3.

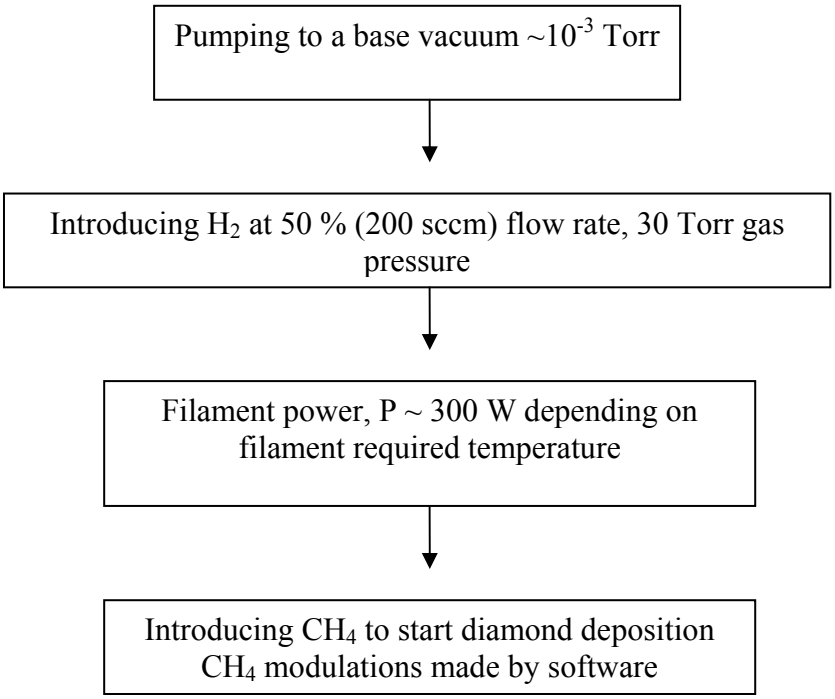

Figure 2.3. Ramp up procedure sequence for diamond deposition using the HFCVD system.

To avoid the effects of atmosphere contamination by undesired gases, the system is pumped to a base vacuum of ~ 10^{-3} Torr and kept at this pressure for around 30 min.

(c) Diamond film deposition. Initially the H_2 gas is introduced in the chamber and the pressure is adjusted. Here, the H_2 flow rate used was 50 % (200 sccm) at a pressure of 30 Torr. The filament temperature software acquisition system and the power source are started, controlling the current (I) and voltage (V) according to the required deposition temperature. The CH_4 is then introduced in the chamber, starting the deposition process. It is well known that diamond nucleation, growth rate and quality depend greatly on deposition conditions [6] and under specific conditions, the film thickness can be easily controlled, by selecting the deposition time [26]. So, the parameters are optimised focusing a required result.

(d) HFCVD system ramp down. The CH_4 is automatically switched off and the power source shut down manually starting the cooling process. The H_2 is switched off and next, the air valve is opened for pressure stabilization.

Before starting the deposition process, the water cooling system is opened. This system is closed after the end of the process. The deposited samples can be taken out from the

chamber, when cooled to room temperature. At this stage, the samples are ready for analysis.

2.2 Scanning Electron Microscopy (SEM)

SEM is an invaluable tool to get a general picture of the coating morphology. SEM is normally employed on the characterization of surface morphologies and cross-section interfaces. Additionally to plan-view, cross-sections of coated samples are regularly studied as they often allow a straightforward observation of the coating morphology, showing size and shape of the columns, cohesion and adhesion to the substrate [3].

The operation consists in scanning a focused electron beam over a material surface and sensing the emission of secondary electrons from it [4]. The detection of the resulting signals allows the acquisition of images, given information regarding topography, chemical composition, atomic number and crystalline structure. When electrons penetrate in the sample, a number of interactions occur that can result in the emission of electrons or photons from, or through, the surface. An illustration of this feature is presented on figure 2.4. A reasonable fraction of the electrons emitted can be collected by appropriate detectors. The output is used to create an image on a cathode ray tube (CRT); where every point that the beam hits on the sample is mapped directly onto a corresponding point on the screen [5].

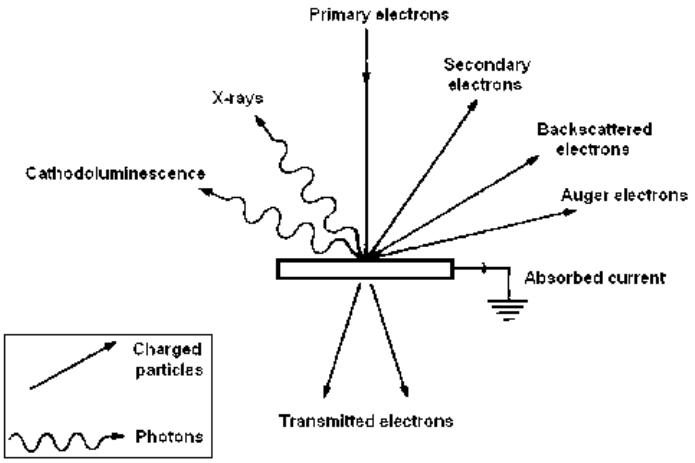

Figure 2.4. Emissions resulting from the bombardment of a sample with an electron beam [7].

The most important images produced in SEM are of three types: secondary electron and backscattered electron images, and elemental X-ray maps. Secondary and backscattered electrons are produced by different mechanisms and the corresponding images are normally separated according to their energies.

Next to secondary and backscattered electrons, the characteristic X-rays produced by the interaction of the electron beam with the sample are the most extensively used signals in a SEM equipment. The X-ray emission signal can be sorted by energy, in an energy dispersive X-ray detector. Its distribution is a characteristic of the elements that originates it, and can be used to produce elemental images representing the spatial distribution of particular elements in the sample.

X-ray mapping is a useful tool for detecting the presence of contaminants, locating inclusions and determining qualitatively or semi-quantitatively the elemental compositions.

In the current work two different equipments were used: a Hitachi S-4100 SEM and a Hitachi SU-70 UHR Schottky FE-SEM systems, in order to examine nucleation and diamond crystal morphology, and also, to verify the adhesion of the deposited films.

Both instruments are equipped with energy dispersive X-ray spectroscopy (EDS), but the SU-70 is a more recent equipment, with superior capabilities. For that reason, the X-ray maps and profiles were assessed with a Bruker AXS Microanalysis GmbH system associated to the SU-70 microscope, due to its high performance and faster acquisition.

The preparation of diamond coated samples for SEM analysis include, frequently, coating the surface with a thin layer of gold or carbon to avoid charging effects [6, 5]. In this study, only the samples that were mounted in cold-setting epoxy resin were coated with a thin layer of carbon.

2.3 Raman Spectroscopy

Raman spectroscopy is a widely used technique to evaluate the types of bonding that are present in carbon films, being a fast and non-destructive method for the characterization of those films, assessing the nature of a film and providing a measurement of the film quality.

The testing procedure consists in a laser that is focused through a microscope onto the surface of a sample and the scattered light is splited into a spectrometer, dispersing it onto

a charge coupled device detector [9]. The work principle is based on the vibrations of the atoms in a crystal lattice at characteristic frequencies.

Lattice vibrations can be visualized as quanta or phonons. A phonon has energy equal to $h.\nu$, where h is Plank's constant and ν is the frequency. In a Raman scattering measurement, monochromatic light with a frequency ν_i interacts with phonons in the crystal with ν_{ph} frequency. At this stage, a phonon can be created originating the Stokes Raman line with ν_i-ν_{ph} frequency, or to the anti-Stokes Raman line, much weaker, with ν_i+ν_{ph} frequency if the phonon is destroyed. The anti-Stokes line depends on the number of excited vibrational levels at an established temperature, and so, being highly temperature dependent. For this reason, normally at room temperature it is the Stokes line that is observed for diamond [6].

The quality of a polycrystalline diamond film can be classified in terms of defects and impurities content between grains, grain size or percentage of non-diamond inclusions [10]. The presence of diamond in CVD films is revealed by a sharp characteristic line positioned at 1332 cm^{-1}, as presented in figure 2.5.

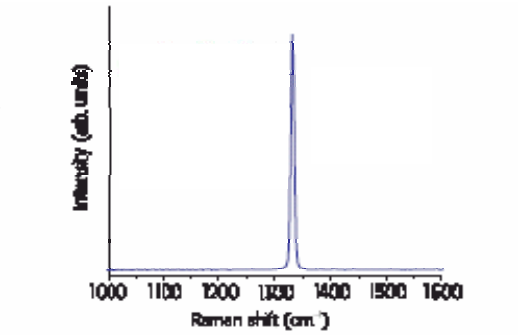

Figure 2.5. Raman spectrum of diamond single crystal (adapted from ref. [9]).

CVD diamond films may also incorporate other carbon species, such as graphite and amorphous carbon. A single crystal of graphite produces a single peak at 1575 cm^{-1} called 'G' peak, while other graphite species present a second peak feature at 1355 cm^{-1} called 'D' peak and representing disordered graphite, as illustrated in figure 2.5. The relative intensity of 'D' peak to 'G' peak is proportional to the presence of 'disordered' carbon and inverse to graphite crystal size [9].

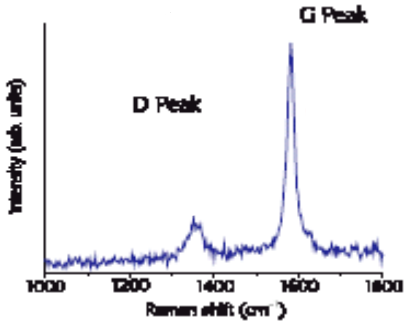

Figure 2.6. Raman spectrum of highly oriented graphite (adapted from ref. [9]).

The ratio between diamond and graphite peak intensities is an indication of the quantity of each phase, although it is also dependent on the excitation wavelength. A commonly used laser wavelength is 514.5 nm green light, from an argon ion laser, but 633 and 785 nm are also frequently used [11].

Experiments on the same diamond coated samples using different laser excitation wavelengths, demonstrate that for smaller wavelengths, non-diamond phase peaks are camouflaged [6, 11]. This phenomenon was attributed to a resonance effect in which non-diamond carbon phases scatter much more effectively at higher excitation wavelengths [6 and ref. within]. As a result, longer wavelengths laser reveals more non-diamond bands, and shorter wavelengths normally leads to a Raman spectra of lower background, with a diamond peak relatively more intense [12].

When characterizing diamond CVD films, the observation of any broad resonance around 'G' peak is generally a signal of the presence of graphite-like non-diamond phases containing sp^2 bonded carbon atoms [13]. Table 2.2 contains a short list of some characteristic Raman scattering bands. An extensive list can be found in L. Pereira work [10].

Table 2.2. Characteristic Raman scattering [10]

Type of carbon	Raman scattering band (cm^{-1})
Diamond precursors (sp^2 disordered carbon)	1140 and 1490
Nanocrystalline diamond	1140, 1150 and 1470
Microcrystalline graphite (D and G bands)	1350 and 1590
High disordered order carbon	1350 and 1600
Diamond-like-carbon (DLC)	1355 and 1580
Microcrystalline graphite	1350, 1580 and 1620
Hexagonal diamond	1326
Natural diamond	1331-1336
Polycrystalline diamond	1333-1345
Polycrystalline graphite	1357
Disordered graphite	1360
Amorphous carbon or DLC	1450-1550 (large bands)
sp^2 amorphous phase structures	1480
Amorphous carbon	1500 (large bands)
Graphite (G band)	1560
Crystalline, hexagonal crystalline and natural graphite	1580
Microcrystalline graphite (D' band)	1613

Micro-Raman spectroscopy was used to first, characterize the deposited diamond films for quality in terms of diamond-carbon phase purity and second, to determine the biaxial stresses developed in the coating during the deposition process.

In this work, the Raman spectrums of the samples were obtained at room temperature, with an ISA Jobin Yvon-SPEX T6400 system with a 514.5 nm Ar^+ ion laser.

2.4 Methods for Residual Stress Evaluation

A quantitative measurement of the residual stress present in a film, is essential to evaluate the effect of the deposition conditions on the system behaviour. Techniques as substrate curvature [14] and X-ray diffraction [15], among others, are used to measure the residual stresses in films.

The residual stresses, developed in diamond films are composed of two different contributions: intrinsic stresses (σ_{in}) and thermal stresses (σ_{th}) [14], as:

$$\sigma = \sigma_{th} + \sigma_{in} \tag{2.1}$$

The film growth process and the thermal expansion mismatch between substrate and film are responsible for those contributions, respectively. Das et al. [16], consider an additional fraction on the equation, related with the lattice mismatch stress, due to the difference in lattice parameter between substrate and film, but equation (2.1) is generally accepted.

A widely used method, based on Raman spectroscopy, was employed on this study, considering that the stresses caused in a film by the mismatch of thermal expansion coefficients, would cause a Raman shift or peak splitting proportional to its magnitude [17].

A single sharp line at 1332 cm^{-1} in the Raman spectrum is an evidence of a good quality polycrystalline diamond film, although the peak is, in general, relatively larger than the one presented by natural diamond and is often slightly shifted in wavelength. Such effects can be attributed to the compressive stress in the film [7].

Various models of stress effects in diamond films have been developed [18 and ref. within]. However, the most common terminology and approach generally found in the literature belongs to Ager and Drory [19]. They developed a general model that allows characterising the residual biaxial stresses in diamond films considering diamond peak shift in Raman spectrum. The model describes quantitatively the relations between singlet or doublet phonon scattering and the biaxial stress σ, measured in GPa, as:

$$\sigma = -1.08(v_s - v_0)\ (GPa) \tag{2.2}$$

$$\sigma = -0.384(v_d - v_0)\ (GPa) \tag{2.3}$$

Equations (2.2) and (2.3) are for single phonon and doublet phonon, respectively. ν_s is the observed maximum frequency of the singlet in the spectrum; ν_d is the maximum frequency of the doublet and ν_0 (= 1332 cm^{-1}), is the characteristic frequency of a unstressed diamond crystal at room temperature. The expressions (2.2) and (2.3) were obtained averaging the relation of stress shift over all crystallite orientations [20].

In many cases, the splitting of Raman line is not obvious, and it is assumed that the observed peak position, ν_m, is located at the centre between the singlet and doublet frequencies ν_s and ν_d, respectively, resulting [21]:

$$v_m = \frac{1}{2}(v_s + v_d) \tag{2.4}$$

Substituting on the equations (2.1) and (2.2), follows:

$$\sigma = -0.567\ \ (v_m - v_0)\ (GPa) \tag{2.5}$$

Using the equations (2.2)-(2.4), the biaxial stress can be calculated.

On the other hand, a theoretical value of the thermal stress can be obtained, according to Ralchenko [21], by:

$$\sigma_{th} = \frac{E}{1-\upsilon}\int_{20^\circ C}^{Tdep}(\alpha_d - \alpha_s)dT \tag{2.6}$$

where E, is the Young's modulus and ν is the Poisson's ratio, of CVD diamond, α_d and α_s are the thermal expansion coefficients for diamond and steel, respectively. The integral is calculated between room and deposition temperatures.

It is desirable for the substrate material to have a low coefficient of thermal expansion. As mentioned before, diamond has one of the lowest coefficients of thermal expansion of any known material: α_d (20 ºC) = 0.8x10^{-6} K^{-1} [22]. Since the CVD growth process occurs at elevated temperatures, upon cooling back to room temperature, the substrate will contract

more than the diamond film, causing compressive stresses in the film. This effect is reflected through the broadening and shifting of the characteristic 1332 cm^{-1} Raman peak of the diamond film. The mismatch in thermal expansion coefficients of diamond and substrate is an important factor to consider, when consider the potential adhesion of a CVD diamond film to a particular substrate material.

2.5 Hardness Testing

Hardness is conventionally measured with indentation testing. Indentation present some associated difficulties when testing good quality CVD diamond films. One fact is that the diamond tip used to make the impression will have a hardness value comparable to that of the film under test. Another aspect is that indent measurements on thin films will only be reliable if proper considerations are given to the contributions from the film and the substrate material [13].

Further considerations on that issue will be done later on this section, but first it will be presented an illustrative description of the type of equipments and principles involved in common macro and micro-hardness measurements.

The hardness tests are generally divided into three types: static indentation test, dynamic hardness test and the scratch hardness test [23]. In this section it is presented a short summary of the procedures and the most important characteristics of hardness testing methods used in this study, which are included on the first category.

The indentation hardness test is most commonly used. Methods such as Vickers and Brinell hardness are here included. Such tests causes a permanent deformation on the test piece, using an indenter that is forced to penetrate into the material with a specific force and the hardness of the test piece is determined, based on the load used to generate the deformation and on the dimensions of the resulting deformation, as penetration depth or indentation area. Vickers and Brinell hardness tests employ the indentation area measurement to calculate hardness.

(A) Brinell Method

Brinell hardness test consists basically in forcing a hardened steel ball or a tungsten carbide (WC) ball with a specified diameter (D) in the surface of a sample, applying gradually a constant force (F) during a specified period of time. After removing the load, the resultant round impression diameter is measured by a low-magnification microscope [23].
The value of Brinell hardness represents the relation between the test force (F) and the area (A) of the impression, expressed by:

$$HB = \frac{1}{g}\frac{F}{A} \quad [N\ mm^{-2}] \tag{2.7}$$

Where g, represents the gravitational constant. The Brinell hardness number (HB) can be calculated according to the simplified equation, as following [24]:

$$HB = \frac{0.102}{\pi D}\frac{2F}{(D-\sqrt{D^2-d^2})} \tag{2.8}$$

where d is the diameter of the indentation. Usually, it is not necessary to do the calculation because HB values are available in the literature, in a tabular form as a function of D, d and F [23, 24].
The depth, in mm, of a Brinell indentation can be calculated from the equation [23]:

$$Depth = \frac{F}{\pi D(HB)} \tag{2.9}$$

Depth calculation is useful to determine the recommended minimum sample thickness for a particular HB. The sample thickness should be at least ten times the depth of the indentation. Other important details for a correct measurement can be mentioned, as: the test must be developed at room temperature; the sample should be fixed; sample surface should be flat and polished; the indentations should be made far enough from the edges of the sample and the spacing between the centres of adjacent indentations should be in the minimum, three times the diameter of the indentation [23].

In this work, a series of indentation tests were performed in a Frank Hardness tester Frankoskop 38180 with a 2.5 mm Brinell steel ball indenter.

(B) Vickers Method

In this test, a Vickers indenter is used, consisting in a diamond tip with the form of a right pyramid with a square base, having an angle of 136º between the opposite faces at the vertex. Vickers hardness number (HV) is determined based on the test force used, when penetrating the Vickers indenter on the sample surface and the indentation area, calculated from the diagonal length of the pyramidal indentation [23]:

$$HV = 2\sin\left(\frac{\theta}{2}\right)\frac{P}{d^2} \tag{2.10}$$

where θ is the angle between opposite faces of the tip (136º), P is the applied load in kgf and d, is the indentation diagonal in mm. Simplifying the expression, comes,

$$HV = 0.1891\frac{F}{d^2} \tag{2.11}$$

where F is the test force in (N) and d, is the mean of the indentation diagonal length in (mm) [24]. One of the major advantages of this method is to allow the determination of the hardness of extremely hard materials, until 1500 HV, impossible to obtain with Brinell test.

(C) Micro-hardness Test

The micro-hardness test is usefully applied in the measurement of the thickness of hardened layers and also, in determining microstructures hardness or the hardness of very thin pieces.

Vickers micro-hardness method is equivalent to Vickers test. A pyramidal diamond tip is used to cause a microscopic impression on the material surface. The applied loads are usually in the range of 10 to 1000 gf.
It should be noted that the indentation depth D is around one-seventh of the indentation diagonal d. There is a dependence relation between hardness and the applied load, mainly in micro-hardness measurements in the range of 1 g to 3 kg, for higher loads the hardness values are constant [1 and ref. within]. Therefore, every hardness measurement should refer the load range.

Knoop method is rather rarely on hardness measurements of thin films, in spite of the lower indent penetration depth, comparing with Vickers, for the same load [36].
Measurements of diamond coatings hardness were made using a Shimadzu micro-hardness tester HMV- 2000 with a Vickers indenter, with loads from 20 g to 1 kg and load application time of 10 sec at normal ambience humidity and temperature conditions. For more accurate measurements, three indentations were made for each load value.
It is very important to notice that for thin coatings, hardness is influenced by the presence of the substrate. The indentation response of a coated system is a complex function of the elastic and plastic properties of both coating and substrate. This effect is marked in the case of diamond coatings on metal substrates and need to be considered when analysing the measured data.

Depth-sensing indentation techniques (DSI), also referred as nanoindentation, have become useful tools on measuring local mechanical behaviour at sub-micrometer scales. Those techniques are essential to assess mechanical properties of thin films, as hardness or small structural features. It is possible to use forces in the order of 1 nN [37]. The analysis of a sample is done based on the indentation load-displacement data.
In spite of the extensive use of nanoindentation to evaluate the hardness of thin films, Vickers and Knoop microindentation methods can be very useful. The nanoindentation contact scales are usually smaller than the film thickness and in this range, the calculated hardness value increases with a decrease in the contact load, known as indentation size effect (ISE) [32]. This means that a hardness value resulting from nanoindentation, is not sufficient to act as a criteria for materials selection, for example. Additionally, for films with a significant surface roughness or deposited on a rough substrate, could be difficult to

achieve reliable and reproducible data from nanoindentation, while microindentation allows an averaging of the surface roughness effect [36].

To extract the value of the film hardness, several methods both experimental and theoretical, have been created either for nano and microhardness scales. A condensed review of some of the main methods will be exposed in the section below.

(D) Models for hardness measurement in coated systems

Ranging from traditional macro-Vickers indentation to ultra-low-load depth sensing nanoindentation [37], is possible to have a hardness response over scales that vary from macroscopic scales where the system behaviour is dominated by the substrate to scales less than the coating thickness, where a coating-dominated response is expected, and a mixed response occurs at intermediate scales. Many studies have been done in the field of hardness measurement of coated systems, and a variety of models were constructed in order to provide a good fit between experimental data above different contact scales and deformation modes.

Usual models for coated systems hardness evaluation are divided in two types: system models and mechanistic models. System models separate the contact response into the contributions of substrate and coating without distinguish between the deformation mechanisms occurring in each of them. Those methods become invalid when big changes such as film cracking occurs during deformation. Mechanistic models consider the effect of a given deformation mechanism on the contact response, but in general, most coated systems present a combination of deformation modes, thus limiting their application.

Jonsson and Hogmark [35] used an area law-of-mixtures approach to model the composite hardness of a substrate/film system. This model was applicable in the cases where a well defined cracking and bending of the film is verified, i.e. at penetration depths usually larger than the film thickness. However, an important feature that characterizes the hardness dependence on load for small indentation sizes, was not explicitly considered in this analysis.

A volume law-of-mixtures hardness model was first suggested by Sargent [30 and ref. within], and further extended by other authors [30 and ref. within]. It is a more generally

applicable model, particularly for very low indentation depths or in the cases where plasticity dominates, i.e. without fracture. Good results were obtained on separating the coating hardness from the composite hardness value. The model demonstrated good applicability for studies on soft films deposited on harder substrates or harder films on softer substrates.

A good review of some of these models and other approaches can be found, for example, on Korsunsky et al. [30, 31 and ref. within].

Although a relatively suitable applicability, all these models are normally restricted to a particular range of loads and are difficult to use. Many studies have been made and big efforts are continuously being done, in order to create satisfactory models, mathematically tractable, allowing simple fitting procedures to be used. Any of the mentioned methods was employed; they are included on the chapter, as complementary information.

2.6 Adhesion Evaluation

In coated systems, the adhesion between coating and substrate is a fundamental requirement for technological applications, so its quantitative evaluation is very important.

Adhesion testing methods can generally be categorised into three types: (a) nucleation methods, based on the measurement of aspects as nucleation rate evaluation and island density, (b) mechanical methods, based on the application of a force onto the coated system, as in pull-off tests [20], scratch-tests [25, 39] or indentation tests [28] and (c) miscellaneous methods, based on indirect methods as X-ray diffraction [14]. The mechanical methods for adhesion have the most practical interest in terms of results, capable of a quantitative evaluation but with some limitations. For instances, pull-off tests are limited by the adhesive strength, normally weaker than 90 MPa [34]. Adhesion scratch tests tend to depend on the coating and substrate materials. In scratch test, the hardness of diamond coating leads to the scratch tip cleavage with its implications in testing repeatability.

SEM analysis of the indented regions, in combination with acoustic emission signals (AES) measurement during loading is a method frequently used to evaluate coating

adhesion [39], by means of a critical load value derived from AES at which initiates the delamination of diamond film.

Micro-indentation testing permits a semi-quantitative evaluation of distinct coatings adhesion, considering the slope of dependent load variation with film spallation radius.
One interesting approach was developed by Fan et al. [33,34], who presented a model to predict quantitatively the adhesion of diamond coating according to the spallation produced by indentation. The authors found, that independently of the shape of the indenter, small indentation loads, up to 100 gf [34], causes round spallation in diamond coatings on metal and proposed an exponential relation for the deformation of the coating under indentation. The coating adhesion is assumed as being equivalent to the deformation stress at the edge of the spallation zone.
In the present study an evaluation of diamond coatings adhesion was done by indentation testing employing a Brinell indenter. A range of indentation loads between 50 and 187.5 kgf where used. Raman spectroscopy was used as a complementary method with the indentation tests, to evaluate the coating adhesion.

References

1. N. Ali, V.F. Neto, and J. Grácio, "Promoting secondary nucleation using methane modulations during diamond chemical vapor deposition to produce smoother, harder, and better quality films", Journal of Materials Research, 18 (2) (2003) 296
2. See f. ex. www.mec.ua.pt/tema/index.html (11.11.2007)
3. N.J.M. Carvalho, "Low Friction and Wear Resistant Coatings – Microstructure and Mechanical Properties", PhD Thesis, Groningen University Press-Netherlands, (2001)
4. H.S. Nalwa, Handbook of Thin Film Materials, Volume 2: Characterization and Spectroscopy of Thin Films, Chapter 3, (2002) 115- 147
5. C. Richard Brundle, Charles A. Evans, Jr. and Shaun Wilson, Encyclopedia of Materials Characterization: surfaces, interfaces, thin films, Butxetworch-Heinemann chapter 2 (1992) 60-99
6. Q.H. Fan, "Diamond deposition on metals", University of Aveiro-Portugal, PhD Thesis (1998)
7. V.F. Neto, "Investigation of the film properties of advanced diamond coatings deposited using time-modulated CVD", MSc dissertation, University of Aveiro, (2004)
8. M. Ohring, Materials Science of Thin Films- deposition and structure, second edition, chapter 10 (2001) 559-640
9. J. Filik, "Raman Spectroscopy: a simple, non-destructive way to characterise diamond and diamond-like materials", SpectroscopyEurope, Volume 17 No. 5 (2005)
10. L. Pereira, "*Propriedades optoelectrónicas de diamante crescido a partir da fase gasosa*", PhD Thesis, University of Aveiro – Portugal (2000)
11. A.O. Lobo, A.A. Martin, E.F. Antunes, V.J. Trava-Airoldi, E.J. Corat, "*Caracterização de materiais carbonosos por espectroscopia Raman*", Revista Brasileira de Aplicações de Vácuo 24 2 (2005) 98-103
12. N. Ali, G. Cabral, A.B. Lopes and J. Grácio, "Time-modulated CVD on 0.8 μm-WC–10%-Co hardmetals: study on diamond nucleation and coating adhesion", Diamond and Related Materials 13 (2004) 495–502
13. M.N.R. Ashfold, P.W.May, C.A.Rego and N.M. Everitt, "Thin film diamond by chemical vapour deposition methods", Chemical Society Reviews, (1994) 21-30

14. S.M.F. Carvalho, "*Propriedades mecânicas e características microestruturais de filmes finos nanocompósitos de (Ti,Al,Si)N preparados por pulverização catódica reactiva em magnetrão*", University of Minho-Portugal, PhD Thesis (2004)
15. E. Liu, L. Li, B. Blanpain and J. P. Celis, "Residual stresses of diamond and diamond like carbon films", Journal of Applied Physics 98 (2005) 073515
16. D. Das, V. Jayaseelan, R. Ramamurti, R.S. Kukreja et al., "Low surface temperature synthesis and characterization of diamond thin films", Diamond and Related Materials 15 (2006) 1336-1349
17. Q.H. Fan, A. Fernandes, E. Pereira and J. Grácio, "Evaluation of biaxial stress in diamond films", Diamond and Related Materials 8 (1999) 645-650
18. E. Anastassakis, "Strain characterization of polycrystalline diamond and silicon systems", Journal Of Applied Physics 86 1 (1999) 249-258
19. J.W. Ager and M.D. Drory, "Quantitative measurement of residual biaxial stress by Raman spectroscopy in diamond grown on a Ti alloy by chemical vapour deposition", Physical Review B 48 (1993) 2601
20. Q.H. Fan, E. Pereira and J. Grácio, "Diamond deposition on copper: studies on nucleation, growth, and adhesion behaviours", Journal of Materials Science 34, (1999) 1353 – 1365
21. V.G. Ralchenko, A.A. Smolin, V.G. Pereverzev, E.D. Obraztsova et al., "Diamond deposition on steel with CVD tungsten intermediate layer", Diamond and Related Materials 4 (1995) 754-758
22. J.C. Bareiβ, G. Hackl, N. Popovska, S.M. Rosiwal, R.F. Singer, "CVD diamond coating of steel on a CVD-TiBN interlayer", Surface & Coatings Technology 201 (2006) 718–723
23. ASM Handbook, Formerly Ninth Edition, Metals Handbook, Volume 8 (1985) 69-109
24. J.P. Davim, A.G. Magalhães, Estante Editora, *Ensaios Mecânicos e Tecnológicos*, Chapter 4, (1992) 56-79
25. S. Schwarz, Y. Musayev, S.M. Rosiwal, C. Schaufler, R.F. Singer and H. Meerkamm, "High temperature diffusion chromizing as a successful method for CVD-diamond coating of steel", Diamond and Related Materials 11 (2002) 757–762
26. T. Chunjiu, "*Hidrogénio em filmes de diamante crescidos por CVD assistido por plasma*", PhD Thesis, University of Aveiro-Portugal, (2004)

27. C.F.M. Borges, E. Pfender, J. Heberlein, "Influence of nitrided and carbonitrided interlayers on enhanced nucleation of diamond on stainless steel 304", Diamond and Related Materials 10 (2001) 1983-1990
28. N. Ali, G. Cabral, E. Titus, A.A. Ogwu and J. Grácio, "Characterization of diamond adhesion on micro-grain WC-Co substrates using Brinell indentations and micro-Raman spectroscopy", Journal of Physics: Condensed Matter 16 (2004) 6661-6674
29. K.V. Dahl, J. Hald & A. Horsewell, "Grey-scale conversion X-ray mapping by EDS of multielement and multiphase layered microstructures", Journal of Microscopy 225 (2006) 31-40
30. A.M. Korsunsky, M.R. McGurk, S.J. Bull and T.F. Page, "On the hardness of coated systems", Surface & Coating Technology 99 (1998) 171-183
31. A.M. Korsunsky, A. Constantinescu, "Work of indentation approach to the analysis of hardness and modulus of thin coatings", Materials Sience and Engineering A 423 (2006) 28-35
32. L. Qian, M.Li, Z. Zhou, H. Yang and X. Shi, "Comparison of nanoindentation hardness to microhardness", Surface & Coatings Technology 195 (2005) 264-271
33. Q.H. Fan, A. Fernandes, E. Pereira and J. Grácio, "Quantitative evaluation of adhesion of diamond coatings", Journal of Materials Research 14 3 (1999) 1142-1147
34. Q.H. Fan, A. Fernandes, E. Pereira and J. Grácio, "Adhesion of diamond coatings on steel and copper with a titanium interlayer", Diamond and Related Materials 8 (1999) 1549-1554
35. B. Jonsson and S. Hogmark, "Hardness measurements of thin films", Thin Solid Films 114 (1984) 257
36. D. Ferro, S.M. Barinov, J.V. Rau, A. Latini, R. Scandurra and B. Brunetti, "Vickers and Knoop hardness of electron beam deposited ZrC and HfC thin films on titanium", Surface & Coatings Technology 200 (2006) 4701–4707
37. R.M.R. Junqueira, M.S. Andrade, C. R.O. Loureiro, V.T.L. Buono, "Mechanical properties of interference thin films on colored stainless steel evaluated by depth-sensing nanoindentation", Surface & Coatings Technology 201 (2006) 2431–2437
38. N.V. Novikov and S.N. Dub, "Hardness and fracture toughness of CVD diamond film", Diamond and Related Materials 5 (1996) 1026-1030

39. J. G. Buijnsters, P. Shankar, W.J.P. van Enckevort, J.J. Schermer and J.J. ter Meulen, “The adhesion of hot-filament CVD diamond films on AISI type 316 austenitic stainless steel", Diamond and Related Materials 13 (2004) 848-857

Chapter 3.

Experimental Results and Discussion

A set of samples with dimensions of 10x10x3 mm square, was prepared as substrates for diamond deposition experiments. Four different types of steel were tested: AISI P20 modified (W.Nr. 1.2738), and 304, 310 and 316 steels, from AISI series 300.
AISI P20 modified, is typically used as a mould steel in the plastic injection industry. The steels AISI 304, AISI 310 and AISI 316, are austenitic stainless steels, differing in chemical composition, as presented on table 3.1 [2].

Table 3.1. Chemical composition of the steels [2]

Steel	C (%)	Si (%)	Mn (%)	Cr (%)	Mo (%)	Ni (%)	S (%)
AISI 304	0.08	1.00	2.00	18.50	-	9.50	-
AISI 310	0.20	1.50	2.00	25.00	-	20.50	-
AISI 316	0.08	1.00	2.00	17.50	2.50	12.00	-
AISI P20mod.	0.37	0.30	1.40	2.00	0.20	1.00	<0.01

Table 3.2 presents some physical properties and mechanical characteristics with relevance for the present study, of all four steels. Also, some common applications of each steel are referred.

Table 3.2. Selection of steel substrate properties and applications [2, 3]

Steel	Brinell Hardness (HB)max.	Coefficient of thermal expansion (500 ºC) [10^{-6}/K]	Applications
P20 mod.	290/330	13.7	Moulds for plastics industry
AISI 304	240	18.0	Chemical and food industry
AISI 310	240	17.0	Valves for corrosive gases, refractory components
AISI 316	240	18.5	Paper, chemical, textile and food industry

All samples were prepared from steel blocks, by cutting and machining processes until the appropriate dimensions were obtained. After this stage, the samples suffer a mechanical polishing with SiC papers, up to 2000 mesh, followed by an ultrasonic cleaning of 5 minutes with isopropanol. Prior to diamond deposition, a commercial PVD CrN interlayer was deposited on the samples. An industrial Microcoat PVD-arc system equipped with a random arc source [5], was used to deposit a layer of CrN with around 2 μm in thickness according to product specifications.

The variations in nucleation density and morphology were observed. The effect of CH_4/H_2 flow rate modulations and temperature variations, during different TMCVD cycles at which samples of different steel substrate were submitted, was evaluated. A measurement of residual stresses developed in continuous diamond films and a study of the adhesion were assessed. The films were examined and characterized by SEM, EDS, Raman spectroscopy and indentation tests, as it will described in the following sections.

CrN interlayer effect

As mentioned earlier, before diamond deposition all the samples were coated with a CrN layer of approximately 2 μm in thickness. Such an interlayer, means to act as a barrier for chemical components diffusion from the bulk steel to the samples surfaces. In order to verify its effectiveness, CrN coated steel samples were analysed in surface by EDS point measurements. As a representative example of the obtained results, figure 3.1 illustrates an EDS analysis of the CrN interlayer surface deposited on a P20 mod. steel sample. A SEM equipment, operating in the energy dispersive X-ray analysis (EDX) mode, enables the identification of elements and its distribution in the film [7].

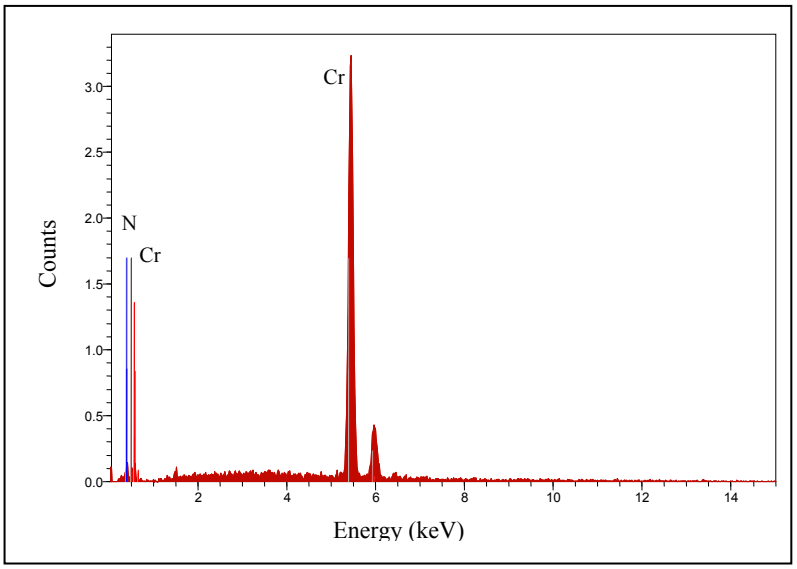

Figure 3.1. EDS of the CrN interlayer surface deposited on a P20 mod. steel sample.

The EDS from the interlayer surface shown a good result in terms of barrier diffusion of elements from the substrate, once the only elements detected were Cr and N, the constitutive elements of the interlayer. It must be noted that the penetration depth of the EDS signal is of about 1 μm.

Samples were also cut transversally to the surface and the cross-sections were analyzed in terms of elemental composition distribution on a section of around 6 μm, measured form the surface to the interior of the sample. As a representative result, in figure 3.2 is shown the X-ray mapping of a P20 mod. steel sample with a CrN layer.

X-ray mapping is a useful tool for detecting the presence of contaminants, locating inclusions and determining qualitatively or semi-quantitatively the elemental compositions. In the present case, the objective of the analysis was to have an idea of the distribution profiles of certain constitutive elements, namely Fe, Cr and C, on the coated system, so a qualitative analysis should be enough elucidative for this propose.

As illustrated in figure 3.2 e), there are well defined layers that define the substrate and the interlayer.

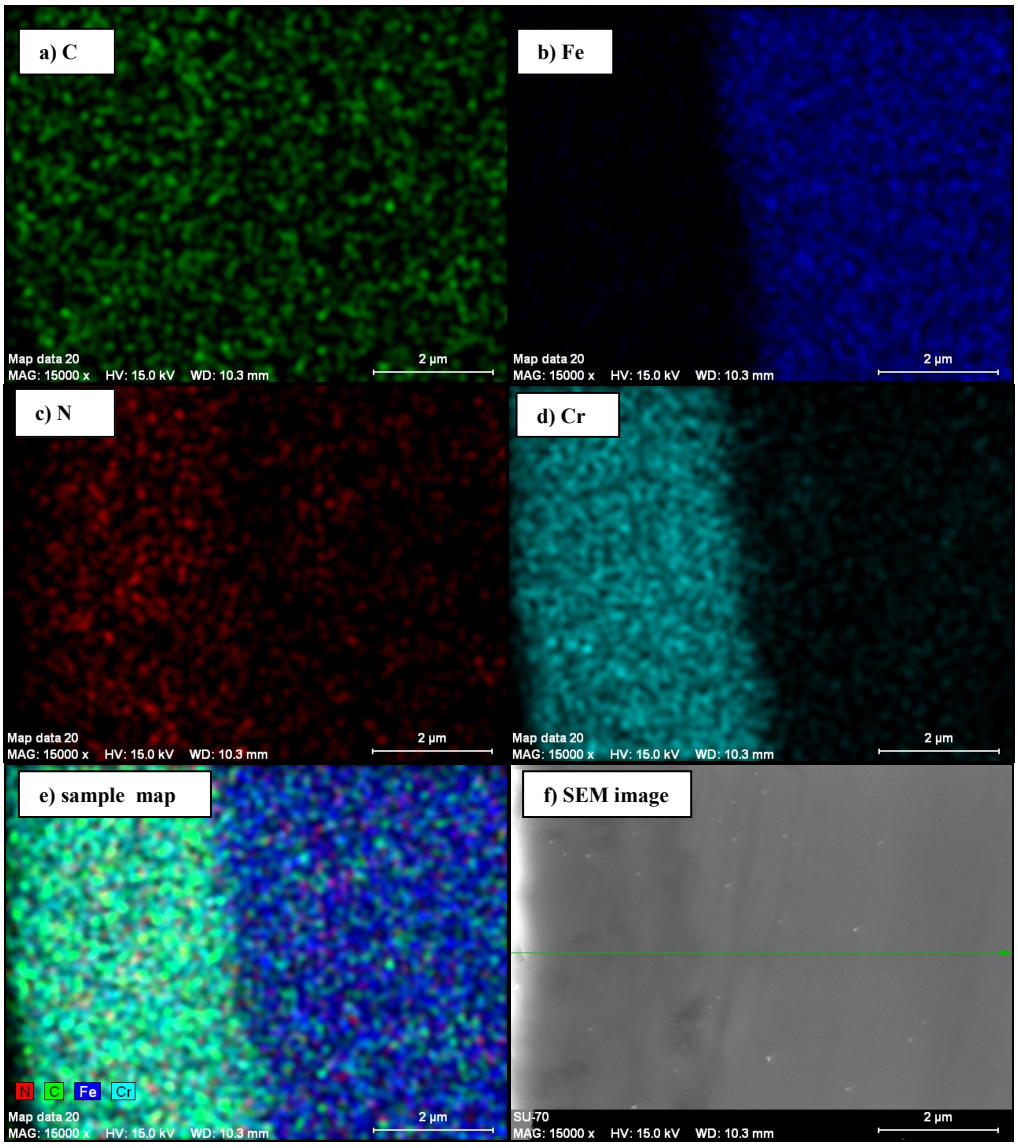

Figure 3.2. X-ray maps of a P20 mod. steel sample with a CrN interlayer. Cross-section images showing each constitutive element distribution (a-d); complete sample map (e) and SEM image (f).

Additionally, an X-ray profile of the same section corresponding to the maps was taken and the result is presented in figure 3.3. The profile represents an average of a measurement on 100 points. This number is a characteristic of the acquisition system. It is possible to confirm the elemental distribution in terms of quality and also, to get a semi-quantitative prediction of each element along the layer in analysis.

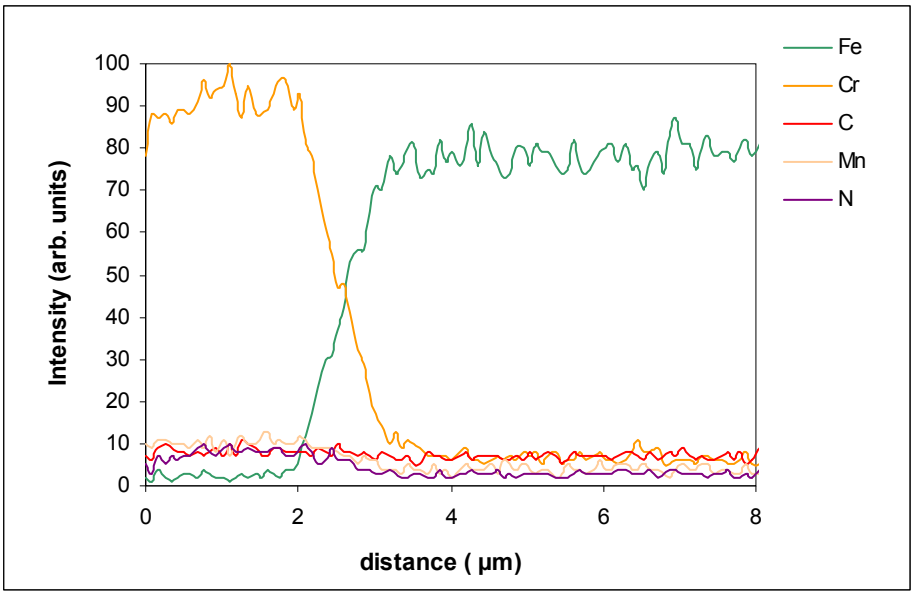

Figure 3.3. X-ray profile of a P20 mod. steel sample with a CrN interlayer.

The high Fe presence in the bottom of CrN layer is a signal of interdiffusion, which means a good bonding between CrN and the substrate, in accordance with J. C. Bareiβ et al. [25].

Study 1. Diamond growth using different TMCVD conditions

Prior to diamond deposition, the samples coated with CrN were ultrasonically abraded during 2.5 hours in a 1/4 µm diamond powder suspension for diamond nucleation seeding, followed by 2 to 3 minutes of ultrasonic cleaning in isopropanol.

To minimize filament contamination of the samples, the Ta filament suffers a pre-carbonization process, using the following conditions: CH_4/H_2 flow rate: 3% (CH_4 flow, 6 sccm; H_2 flow, 200 sccm); time: 30 min; filament temperature: 2100 ºC; gas pressure: 30 Torr. This step allows the formation of a thin layer of tantalum carbide, which besides reducing the sputtering of filament elements to the coating, reduces the filament ductility, preventing its deformation during deposition.

The deposition experiments were conducted in a HFCVD reactor described in chapter 2. During deposition, the filament was kept at a temperature around 2100 ºC, in order to activate the process gases CH_4 and H_2. The deposition parameters are shown in table 3.3.

Table 3.3. TMCVD deposition parameters

Parameter	Value
Pressure (Torr)	30
Filament Power (W)	~ 300
H_2 flow rate (sccm)	200
CH_4/H_2 flow modulations (%)	3, 4

An optimization of diamond deposition parameters, as deposition temperature, methane modulation and deposition time, was attempted. The variation of parameters for TMCVD different cycles is summarised on table 3.4.

Table 3.4. TMCVD parameters for different experimental cycles

Cycle	CH_4/H_2 flow (%)	Depos. time (min)	CH_4 mod. time (min)	CH_4 mod. time (sccm)	Substrate temp. (ºC)
C5	1	161	15 (x2)	6	~ 700
C1	1	281	15 (x2)	8	~ 700, 800
C2	1	281	15 (x2)	6	~ 700, 800
C7	1	400	10 (x3)	6	~ 700
C8	1	415	15 (x3)	6	~ 700
C4	1	551	15 (x4)	6	~ 800

In the table above the cycles are presented for deposition time increasing order. In the following section, a comparison between the results obtained in different deposition treatments will be presented, considering other parameters involved.

To simplify the samples identification, table 3.5 shows a correlation between substrate material and deposition cycle, with a symbolic designation for each sample, which will be used from now on.

Table 3.5. Symbolic identification of samples

Sample	Substrate	Cycle
SP20Mx	P20 mod.	Cx
S304x	304	Cx
S310x	310	Cx
S316x	316	Cx

A) Nucleation density and morphological analysis

Figure 3.4 illustrates the nucleation densities resulting on each sample surface, after submission to the deposition cycles C1, C2 and C5. The cycle C5 consists of CH_4/H_2 modulations at 3% (6 sccm CH_4) during 15 min, follow by 60 min of growing at 1% CH_4/H_2 (2 sccm CH_4), repeated two times. The total deposition time was of 161 min.
Cycles C1 and C2 are characterised by CH_4/H_2 modulations at 4% (8 sccm CH_4) and 3% (6 sccm CH_4), respectively, during 15 min. These modulations were repeated two times, completing a total deposition time of 281 min. Both cycles had growing times of 120 min at 1% CH_4/H_2 (2 sccm CH_4), after each CH_4 modulation.

In the beginning of each deposition process, the samples were submitted to a period of 10 min at 0.5 % CH_4/H_2 (1 sccm CH_4), with two functions associated: first, to stabilize the deposition system in terms of atmosphere and temperature; and second, to promote some surface etching before the nucleation of the first diamond crystallites. At the final stage of deposition, all the cycles comprise a final minute at low CH_4 concentration, in order to achieve a surface etching of the deposited film. The substrate temperature was kept around 700 ºC, by adjusting the filament temperature and regulating the filament-substrate temperature.

Samples of each one of the steels were submitted to the deposition cycle C1. Figure 3.4, presents only the results of S3041, S3101 and S3161. The sample SP20M1 presented a continuous film, but under the cooling process it delaminated almost completely.

As expected, comparing C1 and C2 nucleation densities, higher CH_4 concentration leads to higher nucleation density. Also, from figure 3.4 (b) and (h), we can assume that the difference in crystallite sizes could be due to the increasing in deposition time, between C1 and C5. The better surface coverage on both samples (e) and (f) in relation to (g) and (h), should be related either to the increase on secondary nucleation and enlarge of the deposition time in C2 cycle. The rate of secondary nucleation is expected to increase with deposition temperature [12] and with higher CH_4 flow modulations [27].

In the sample SP20M2 from figure (e), a cauliflower-type or 'ballas' structure can be observed. The formation of this structure seems to be possible, due to the increase of CH_4 concentration during deposition. According to Ali et al. [27], increasing the CH_4 concentration, crystal sizes decrease until over 3% CH_4/H_2 and the crystalline morphology disappears. Such an effect, which origins a nanocrystalline or 'ballas' diamond film, could be considered an aggregate of diamond nanocrystals and disordered graphite.
It is possible to verify that both samples SP20M5 and S3045 present the same (100) and (111) crystal morphology. In the case of sample SP20M5, the nucleation density was higher and with smaller crystals than sample S3045. Also, secondary nucleation could be observable in both samples.

After the first studies on AISI 310 and 316 steel samples, that presented the worst results in terms of diamond nucleation, for the experimental conditions in use, those materials were abandoned. A possible explanation for those results can be related with some chemical composition effect of these materials.

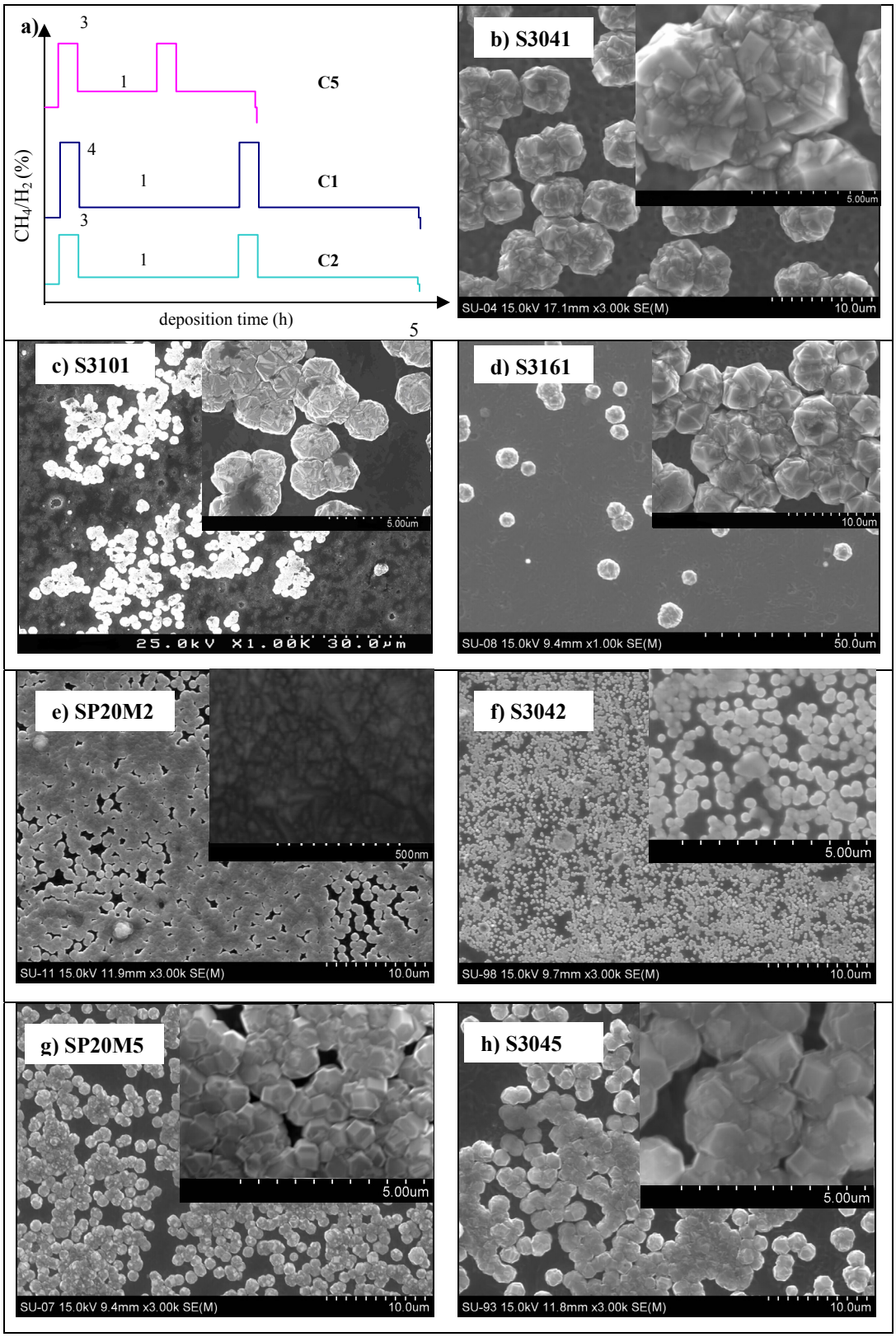

Figure 3.4. Time-modulation of CH_4 in cycles C5, C1 and C2 (a); SEM images showing the density of diamond crystallites in the samples surfaces: (b) S3041; (c) S3101; (d) S3161; SP20M2 (e); S3042 (f); SP20M5 (g) and S3045 (h) samples.

The same cycles C1 and C2, were applied on SP20M and S304 samples, changing the deposition temperature to around 800 ºC. Also, the samples seeding time was increased to 3 hours. The results can be seen in figure 3.5 (b, c). Both samples presented well grown and continuous films. The difference between grain size in both samples can be attributed to the higher CH_4 flow rate modulations in the cycle C1, which could lead to a decrease of crystal size. The secondary nucleation density is expected to be greater for highest CH_4 pulses, because for higher CH_4 concentrations, more C-containing radicals are present in the reactor, then favouring the growth process by initiating diamond nucleation [15].

Both samples S3041 and S3042 completely delaminated after cooling, what could be attributed to the largest thermal expansion coefficient of this substrate material.

Figure 3.5 (d) illustrates the cycle C4, with CH_4/H_2 modulations at 3% (6 sccm CH_4) during 15 min, repeated four times, with a total deposition time of 551 min. The substrate temperature was kept around 800 ºC. Sample SP20M4 shown a continuous diamond film, as revealed in figure 3.5 (e). All the samples present predominance of (111) crystals, better defined on SP20M4 sample.

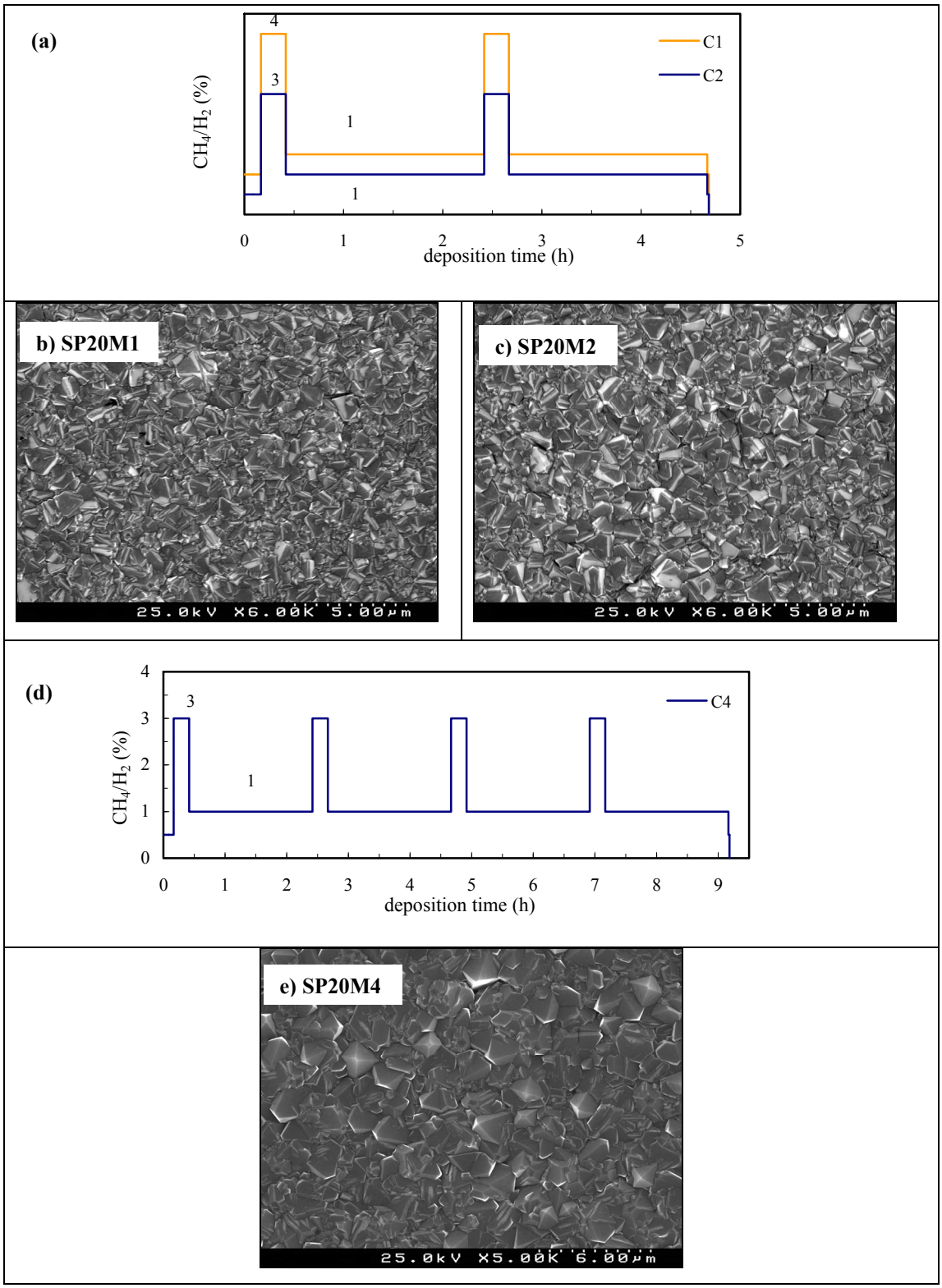

Figure 3.5. Diamond growing during time-modulation of CH_4 in cycle C1, C2 and C4 (a, d); (b) SP20M1; (c) SP20M2 and (e) SP20M4 samples at around 800 ºC.

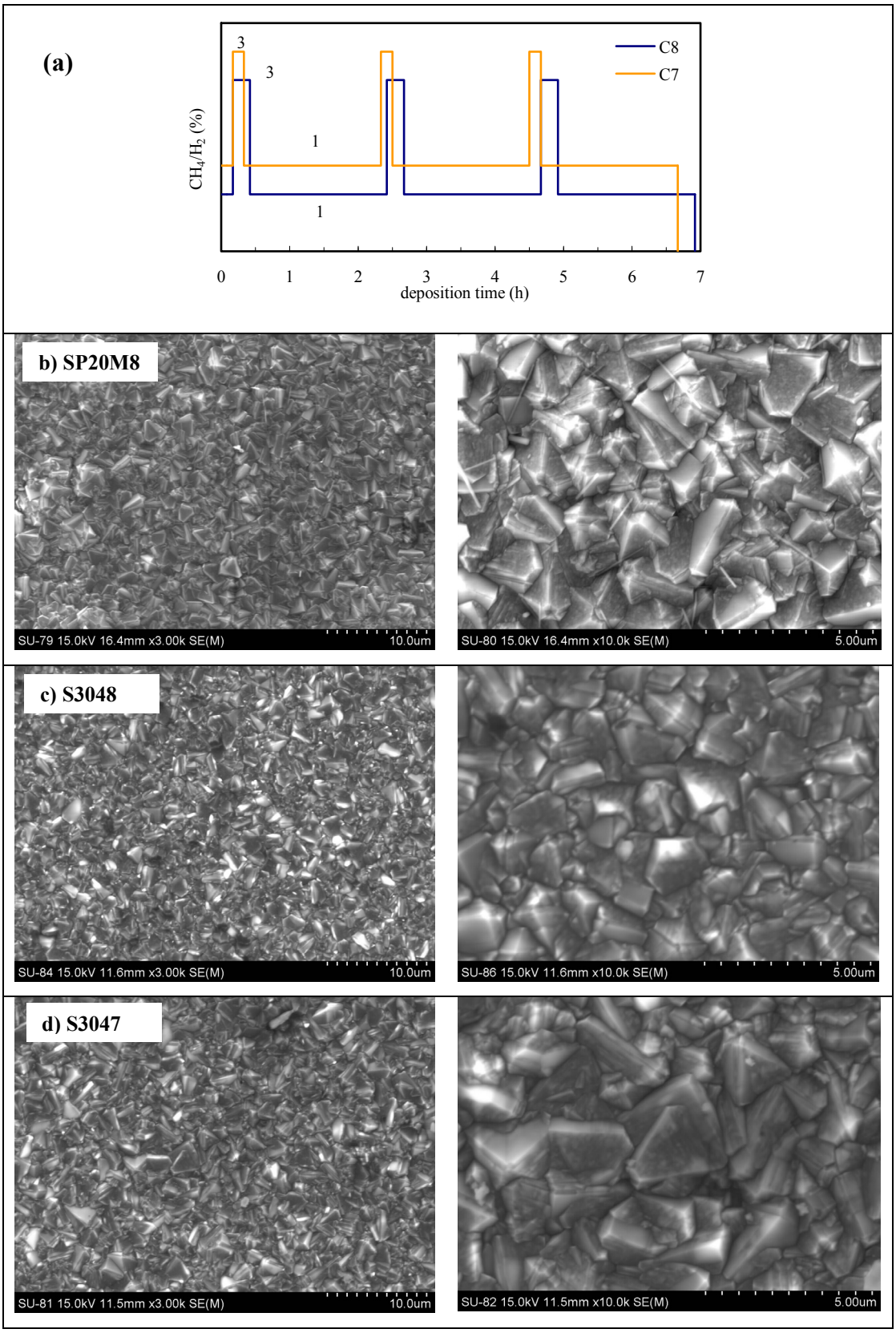

Figure 3.6. Time-modulation of CH_4 in cycles C7 and C8 (a); SEM images showing the diamond growth in SP20M8 (b); S3048 (c) and S3047 (c) samples, with two different magnifications.

Figure 3.6, shows the diamond growing results, through the deposition cycle C8, with CH_4/H_2 modulations at 3% (6 sccm CH_4) during 15 min, repeated three times, with a total deposition time of 415 min. For comparison, in the same figure is presented the cycle C7, with CH_4/H_2 modulations at 3% (6 sccm CH_4) during 10 min, repeated three times, with a total deposition time of 400 min. The substrate temperature was kept around 700 ºC in both deposition processes.

SEM images demonstrate both two effects; first, longer CH_4 modulations should lead to smaller grain sizes, even for the same flow rates, what could be attributed to an increase of secondary nucleation on C8. Secondly, all the samples present well defined (111) crystals. In both cycles, the initial stage at low CH_4 flow rate, included on the previous cycles, was eliminated. The results could be indicative that this stage should not be decisive on the diamond film growth.

B) CrN interlayer behaviour during deposition

The effectiveness of the interlayer during deposition, is shown in figure 3.7, that presents the X-ray mapping of a P20M sample after deposition cycle C1. The sample was cut transversally to the surface and mounted in cold-setting epoxy resin with the cut face up to the top and polished with SiC paper to a mirror finishing.

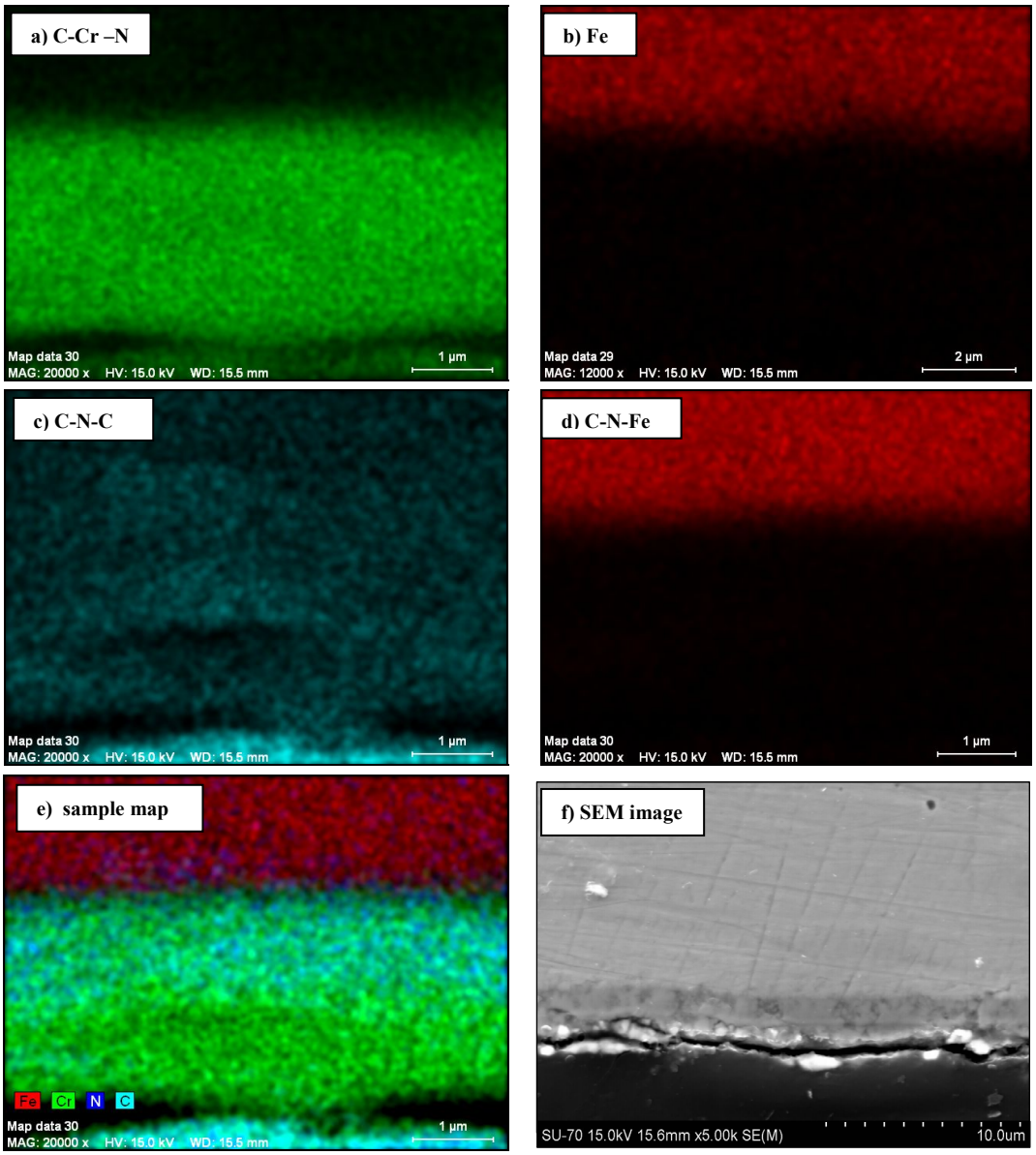

Figure 3.7. Cross-section images showing the constitutive elements distribution of a P20M1 sample.

A similar procedure was adopted for stainless steel samples. Figure 3.8 presents an example of the results obtained for a S304 sample, after the deposition cycle C8. Namely, the depth profiles of the elemental distribution of C, Cr and Fe, assessed by X-ray mapping of sample S3048, are shown in the figure.

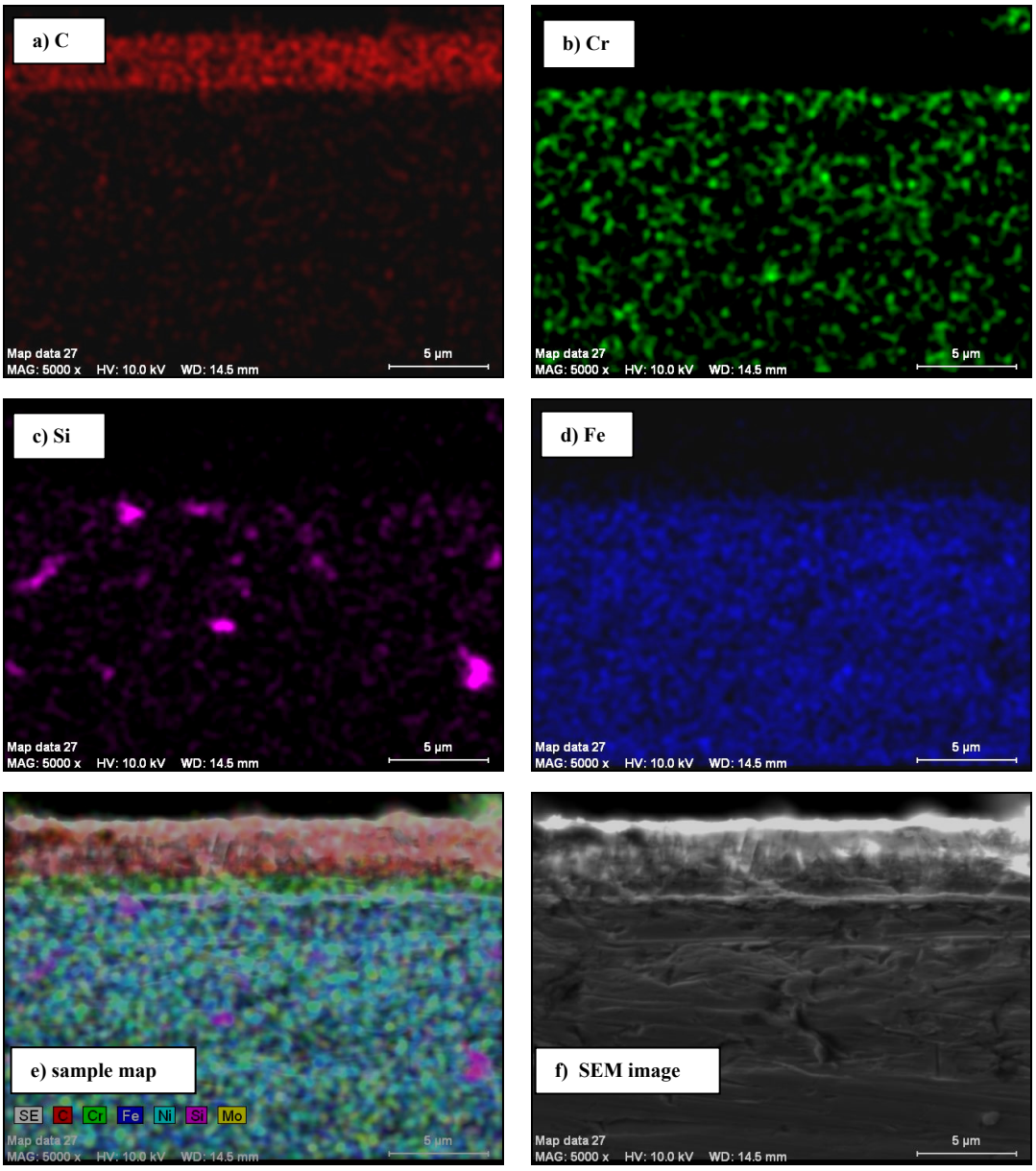

Figure 3.8. Cross-section images showing the constitutive elements distribution of the S3048 sample.

The Fe concentration decreases rapidly at the steel/CrN interface when Cr, N increase. At the diamond/CrN interface Fe is scarcely detectable. These data show that the CrN interlayer constitute an effective barrier from Fe and C diffusion during diamond deposition. Additionally, an X-ray profile of the same section was taken, and the result is presented in figure 3.9.

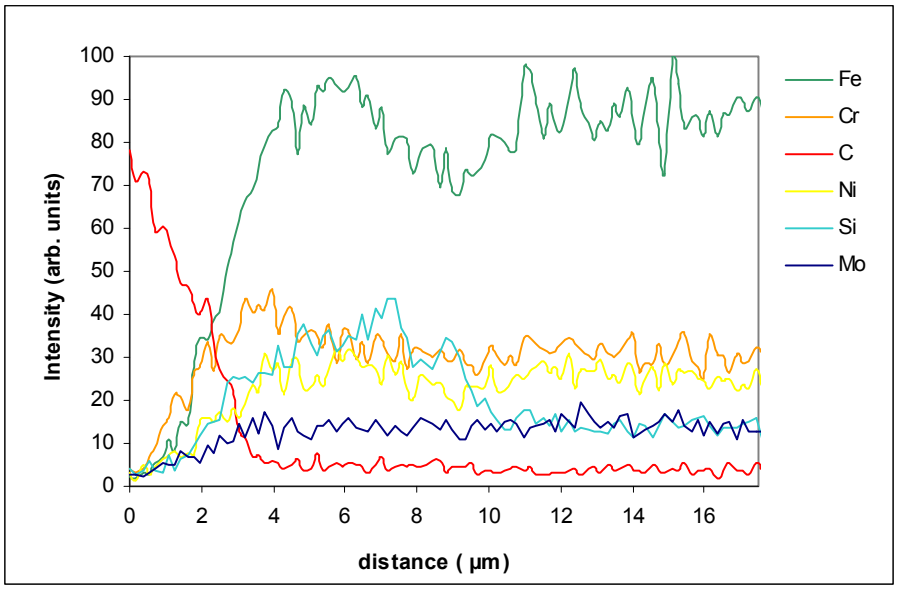

Figure 3.9. Cross-section X-ray profile of the sample S3048.

Study 2. Evaluation of residual stress

A) Residual stress on P20 modified samples

The samples SP20M2 and SP20M4, were analysed by Raman spectroscopy in terms of residual stresses on the films. The deposition conditions of cycles C2 and C4, are illustrated on figure 3.10. Figures 3.11, shows the Raman spectrum of the diamond films.

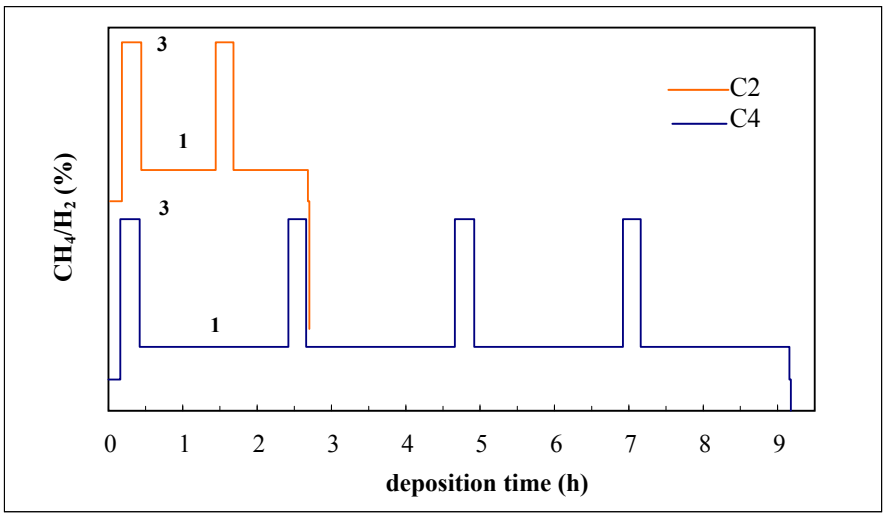

Figure 3.10. Diamond deposition cycles C2 and C4.

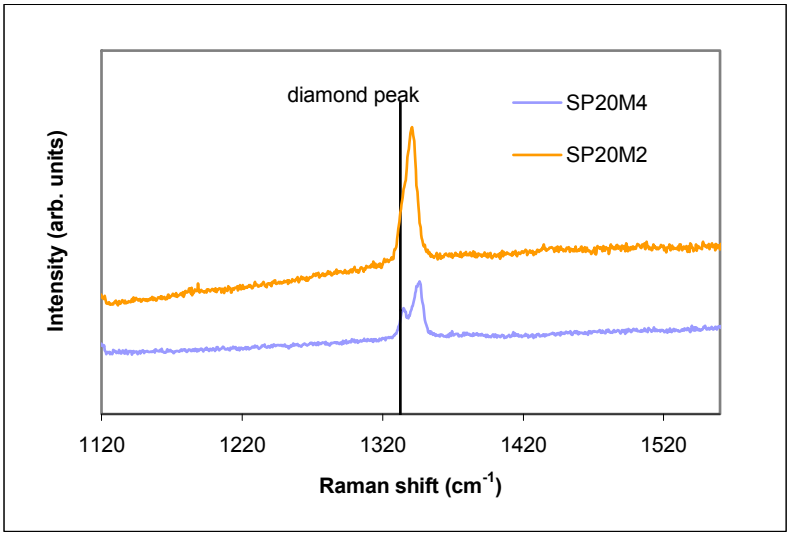

Figure 3.11. Raman spectrum of diamond film grown on samples SP20M2 and SP20M4.

Raman spectra taken from the diamond coatings revealed a shift of the diamond peak, usually positioned at 1332 cm^{-1} to higher wavenumbers, on both samples. This feature may be attributed to the existence of compressive stresses in the films, believed to be caused by the mismatch of thermal expansion coefficients of substrate and film [9]. The value of the stress should be proportional to the diamond peak shift. Additionally, sample SP20M4 present a peak splitting in two components, that could be attributed to the large compressive in-plane stress present in the film [14].

Using the model of Ager and Drory [14], exposed on chapter 2, the biaxial stress σ can be calculated for sample SP20M4, as follows:

$$\sigma = -1.08(\nu_s - \nu_0) \qquad \text{for singlet} \qquad (3.1)$$

$$\sigma = -0.384(\nu_d - \nu_0) \qquad \text{for doublet} \qquad (3.2)$$

where ν_s is the observed maximum frequency of the singlet in the spectrum; ν_d *is* the maximum frequency of the doublet and ν_0 = 1332 cm^{-1} .

In sample SP20M2, the splitting of Raman line is not obvious, and it could be assumed that the observed peak position, ν_m, is located at the centre between the singlet and doublet frequencies ν_s and ν_d [17]:

$$v_m = \frac{1}{2}(v_s + v_d) \tag{3.3}$$

So the biaxial stress σ can be calculated by the equation:

$$\sigma = -0.567 \ \ (v_m - v_0)\,(GPa) \tag{3.4}$$

Table 3.6 summarizes the results on the two samples in terms of residual stresses, assessed by analysis from the Raman spectra.

Table 3.6. Raman peak positions for SP20M2 and SP20M4 samples

Sample	SP20M2	SP20M4
Raman peak shape/position	Single 1342	Split 1346 1336
Biaxial stress (GPa) (from Raman shift)	- 5.67	- 5.37 - 4.32

It is assumed that the stress are constant along the film depth. Although, it was found that Raman spectrum position and shape depends on the film thickness.
In this case, the films thicknesses were not evaluated, but assuming a direct proportionality between deposition time and film thickness, it would be expected that SP20M4 had a highest value and for so, a higher value of residual stresses, promoting the splitting of the diamond Raman speak.

The mismatch of thermal expansion coefficients of steel substrate and diamond film, can be the cause of compressive stress in the coating after the cooling process. CrN has a thermal expansion coefficient similar to diamond, from which its application as an interlayer is expected to develop low residual thermal stresses in the diamond film. Then, assuming that the CrN intermediate layer does not affect significantly the stress development in the diamond film, the theoretical value of thermal stresses can be obtain according to the equation [17]:

$$\sigma_{th} = \frac{E}{1-\upsilon}\int_{T_2}^{T_1}(\alpha_d - \alpha_s)dT \quad (3.5)$$

Where E = 1143 GPa and ν = 0.07 [19] are Young's modulus and Poisson's ratio, for diamond. T_1 (~ 20 ºC) and T_2 (~ 800 ºC), are the room and deposition temperatures, respectively. The thermal expansion coefficients for diamond film at room and deposition temperatures can be found at α_d (20 ºC) = 0.8x10^{-6} K^{-1}; α_d (~ 800 ºC) = 4.5x10^{-6} K^{-1} [17]. For P20 modified steel substrate: α_s (20 ºC) = 11.7x 10^{-6} K^{-1}; α_s (~ 800 ºC) = 14.0 x 10^{-6} K^{-1} [3]. Since α_d and α_s varies with temperature, using specific values for a particular temperature can associate errors to the results. A suitable solution for the question is to plot that variation and fit the values to a second degree polynomial equation [18]. According to A. Fernandes et al. [19], it is reliable to estimate the thermal stress, considering a ΔT interval, between (T_2) and (T_1), and using average values of α_d and α_s for those temperatures, as:

$$\sigma_{th} = \frac{E}{1-\upsilon}(\alpha_d - \alpha_s)\Delta T \quad (3.6)$$

From equation (3.6), a compressive stress value of – 9.78 GPa was determined for the thermal stresses on SP20 samples.

The measured value from Raman spectra, is much lower than the theoretical, that may be caused by some substrate surface structural effect. The shift of diamond Raman peak to higher wavenumbers indicate an increase of residual stress in the film with the deposition time, in agreement with previous results obtained for CVD diamond films on steel substrates [20,21].

Furthermore, the Raman spectrum of films with different deposition times presents a very similar shifting of diamond peak. In agreement with Polini et al. [21], for higher deposition times in terms of comparison, could be verified a slight shift to higher wavenumbers, that may reveal wider stress distribution with the film thickness increase.

Thermal stresses increases with the decrease in substrate temperature until room temperature, implying that during the post cooling procedure, thermal stress in the diamond film increases. When σ_{th} is much higher than that obtained from the shift of the

diamond Raman peak, what seems to be the case, is a signal that the stress in the film is released [9].

B) Residual stress on AISI 304 samples

As observed from figure 3.12, the Raman spectrum displays a diamond peak at 1338 cm^{-1}. Also, a peak positioned at 1363 cm^{-1} can be detected, that could be associated with amorphous carbon phases present in the film.

In all the samples analysis, was used a micro-Raman system with 514 nm laser wavelength. From the literature, it is known that at this wavelength, non-diamond carbon phases scatter more effectively than diamond due to a resonance effect [12], which may explain the intensity relation between the two peaks from the Raman spectra.

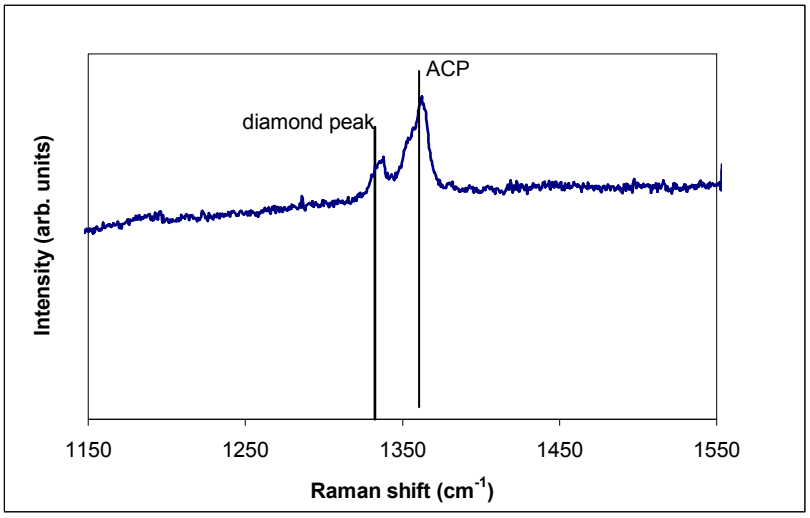

Figure 3.12. Raman spectrum from diamond film grown on S3048 sample.

Table 3.7 summarizes the results in terms of residual stress, assessed by analysis from the Raman spectra and the values obtained for residual stress, according to equations 3.4 and 3.6.

Table 3.7. Raman peak position from sample S3048

Sample	**S3048**
Raman peak shape/position	Single 1338
Biaxial stress (GPa) (from Raman shift)	- 3.42
Thermal stress (GPa)	- 12.83

The substrates have a much larger thermal expansion coefficient (α_s) than diamond and as a result, it is expected a large thermal stress in the film. As previously explained, those stresses can cause a Raman shift or peak splitting. However, considering the values of α_s for S304 and SP20M, it could be expected that the diamond film deposited on 304 steel, developed larger thermal stress.

Study 3. Measurement of film adhesion

The coated samples were indented in different locations using various loads. Raman spectroscopy was employed as a complementary method to evaluate the coating adhesion by assessing the stress level variations or relief.

The diamond films adhesion to substrate was evaluated by an indentation technique using Brinell hardness tests. The adhesion strength was assessed by the measurement of the load applied to the indenter, necessary to induce delamination and fracture of the diamond films.

A) Diamond coating adhesion on P20 modified samples

Indentation tests were performed with loads ranging from 50 to 500 gf. Through this indentation load range, the films did not crack. The stress levels were measured at specific points on the indented samples. Figures 3.13 and 3.14 illustrate the results obtained on the samples SP20M2 and SP20M4 before and after indentation.

Before indentation tests, Raman spectra of both films deposited on SP20M2 and SP20M4, showed a diamond peak at wave numbers higher than 1332 cm^{-1}, indicative of the adhesion between diamond coating and substrate, and consequently the existence of compressive stresses in the films, mainly, due to the different thermal expansion coefficient between substrate and film.

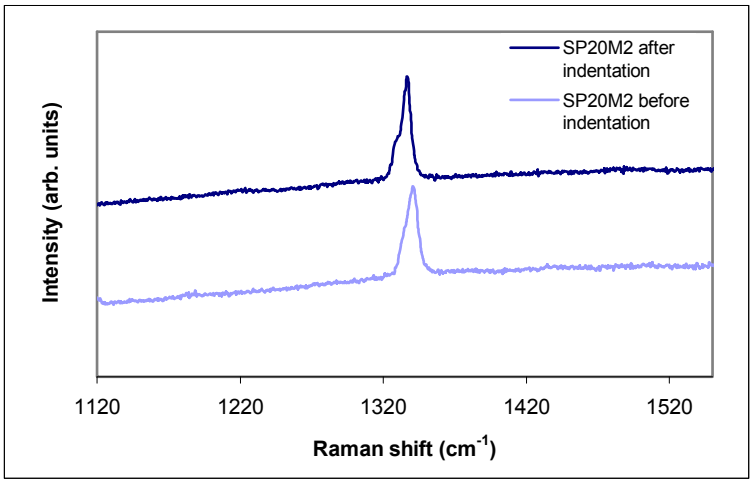

Figure 3.13. Raman spectrum from diamond films grown on SP20M2 sample before and after indentation.

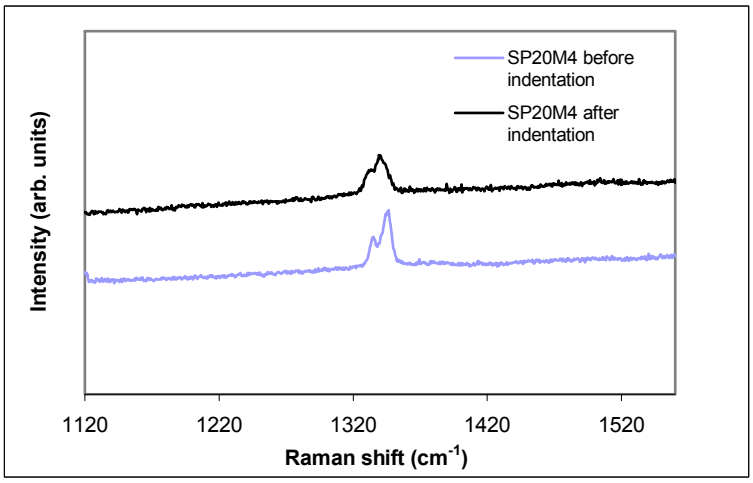

Figure 3.14. Raman spectrum from diamond films grown on SP20M4 sample before and after indentation.

After indentation, the Raman spectras corresponding to the indentation border zone, present a peak closer to 1332 cm^{-1}. This feature demonstrate a stress relieve of the films

after indentation as it detached from the substrate [26]. Such an effect seems to have a very similar magnitude in both samples. Table 3.8 summarized these results.

Table 3.8. Raman peak positions before and after indentation of the samples SP20M2 and SP20M4

Sample	**SP20M2**	**SP20M4**	**Biaxial stress (GPa)**
Raman peak shape/position	Single	Split	
before indentation	1342	1336 1346	- 5.67 - 4.32 - 5.37
after indentation	1337	1334 1340	- 2.84 - 2.16 - 3.07

A series of Brinell indentations with loads ranging from 10 to 187.5 kgf was also performed. SEM images from indentation at various loads of samples SP20M2 and SP20M4, are presented on figure 3.15 and 3.16. Results showed no visible delamination occurring up to a load of 125 kgf.

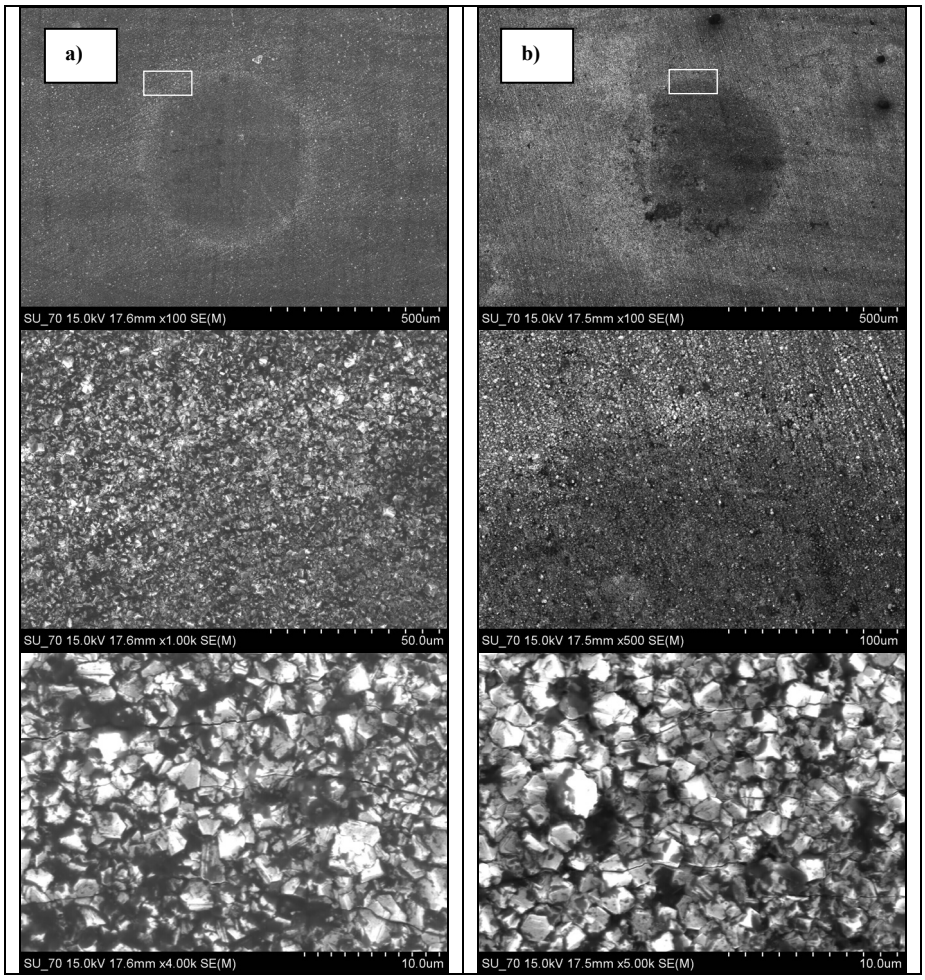

Figure 3.15. SEM images from Brinell indentations of samples SP20M2 (a) and SP20M4 (b) at 125 kgf at different magnifications.

After indentation, it becomes visible a white spallation area around the indentations. This feature demonstrates that after indentation, the film detached from the substrate [26]. In both samples, it could be observed small intergranular concentric cracks.

According with Novikov and Dub [31], the absence of radial cracks emanating from the concentric cracks, could be explained with a high level of internal compressive stresses in the diamond film.

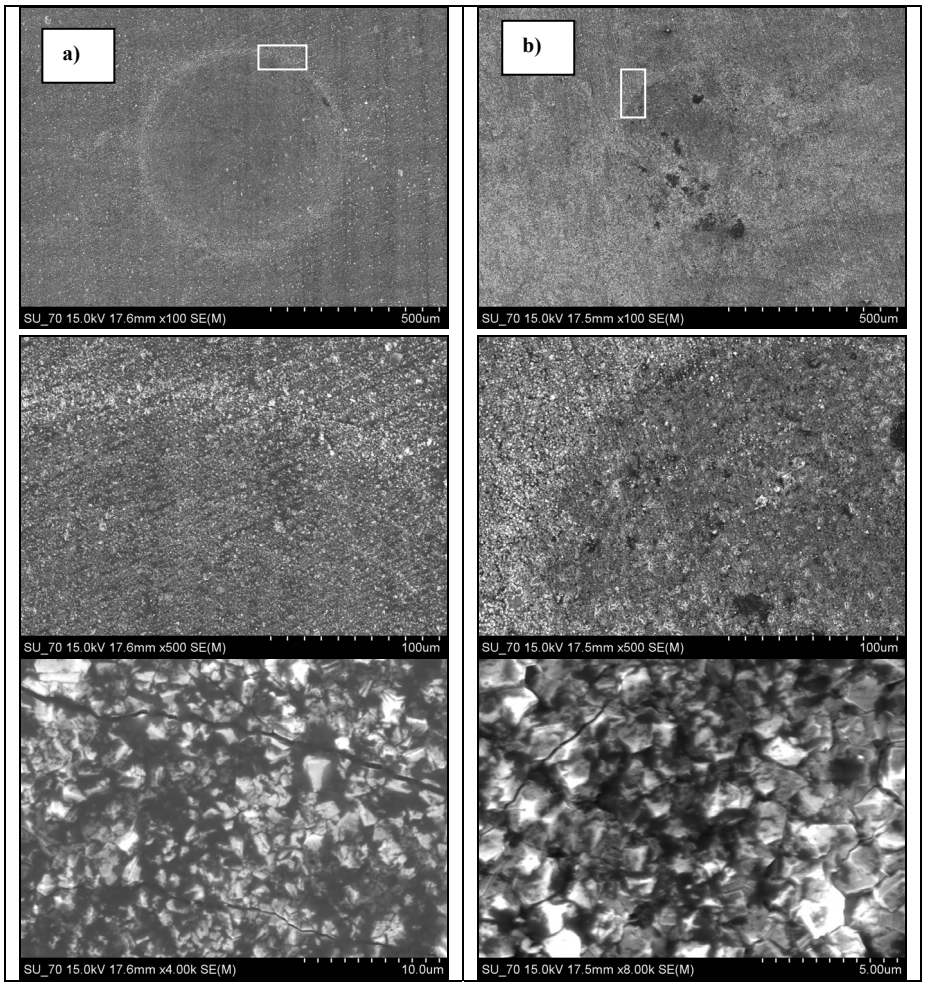

Figure 3.16. SEM images from Brinell indentations of samples SP20M2 (a) and SP20M4 (b) at 187.5 kgf at different magnifications.

At a superior load, as shown in figure 3.16, more pronounced concentric cracks are present and the films delamination is evident.

From the images of the surface region near the boundary of the indentation, it is visible either inter and intragranular cracks. From these results it is possible to expect that the film delamination starts on both samples, at indentation loads up to 125 kgf.

B) Diamond coating adhesion on AISI 304 samples

The indentation tests were performed with the same load range that for SP20M samples, between 50 to 500 gf. Figure 3.17 illustrates the Raman results obtained on the sample S3048 before and after indentation at the higher indentation load. The spectra were taken in the border of the indent.

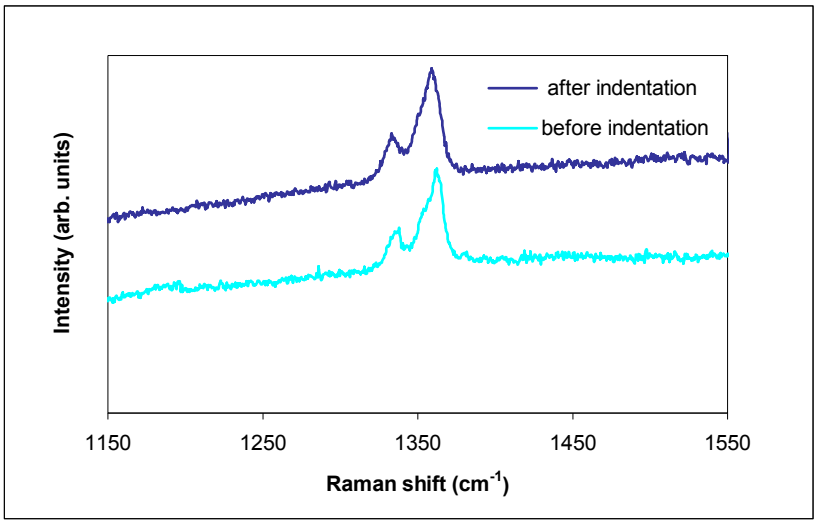

Figure 3.17. Raman spectrum from diamond films grown on S3048 sample, before and after indentation.

After indentation, the diamond peak moved to a lower wave number, closer to 1332 cm^{-1}, indicating a stress relieved and film detachment from the substrate. Table 3.9 summarizes the results in terms of stress relieve.

Table 3.9. Raman peak positions before and after indentation of sample S3048

Raman peak position	**S3048**	**Biaxial stress (GPa)**
before indentation	1338	- 3.42
after indentation	1335	-1.70

A series of Brinell indentations with loads ranging from 10 to 187.5 kgf were performed. SEM images from indentation at various loads of sample S3048, are presented on figure 3.18.

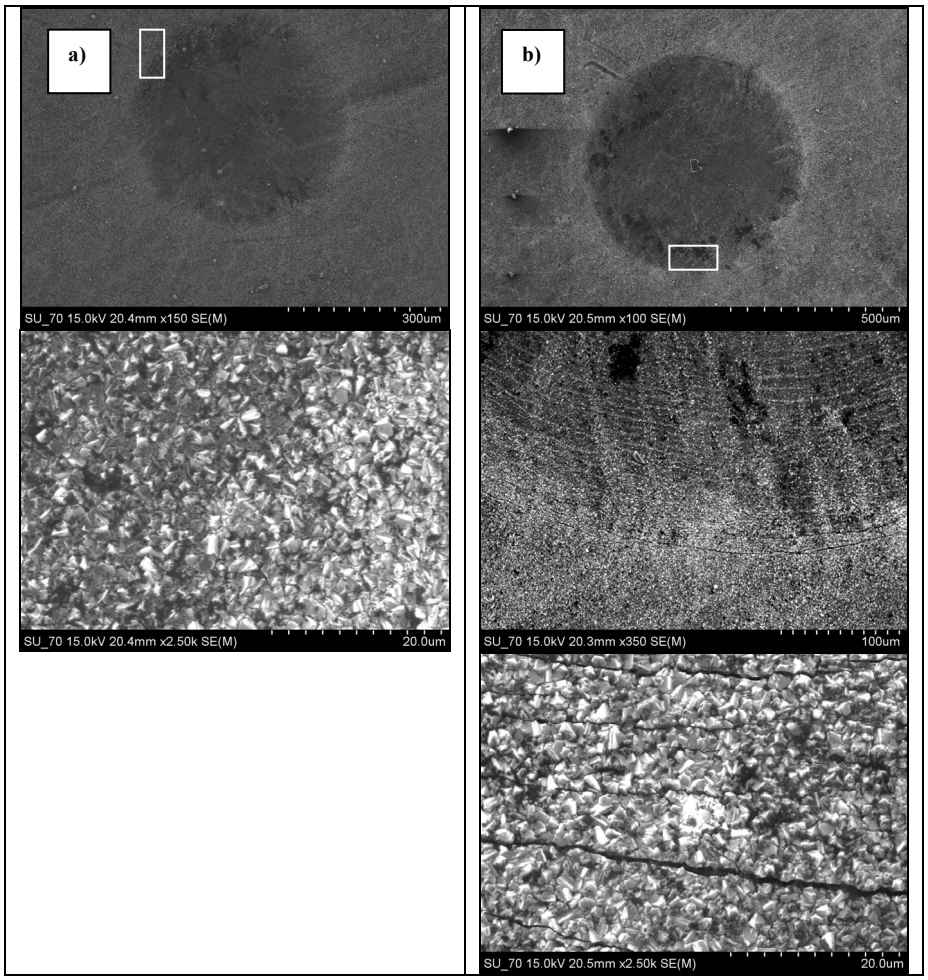

Figure 3.18. SEM images from Brinell indentations of sample S3048 at 20 kgf (a); 50 kgf (b) at different magnifications.

The coated samples deformed to the shape of the indenter, what could be explained by the expected plastic deformation of the steel substrates during indentation.

For loads from 10 kgf and 20 kgf, no cracks or delamination of the diamond film can be observed. SEM observations of the indented regions reveal that the film should begin to delaminate between 20 kgf and 50 kgf applied loads. From the images of the surface region near the boundary of the 50 kgf indentation load, it is visible either inter and intragranular fine concentric cracks. It is expected that the film detaches from the substrate in a zone

were the interface strength is smaller than the deformation stress caused by the indentation [26].

Due to the columnar growth characteristic of polycrystalline diamond films, when a crack occurs on the surface of the film, it tends to propagate through the columnar particles, leading to a decrease in toughness [30]. Although, in the case of multilayered films, as the ones resulting from TMCVD, the interfaces formed in this structures are expected to minimize the crack propagation.

Comparing the results obtained from the different sample substrates, it is possible to assume that for S304 samples, the films cracked for inferior loads than in the case of SP20M samples, which could be related to a pronounced effect of the substrate in the S304 samples.

Study 4. Hardness profiles of coated systems

A) Hardness measurements on P20 modified samples

A series of Vickers micro-hardness tests were made in the samples SP20M2 and SP20M4. The results for 200 gf and 500 gf loads are present in figure 3.19.

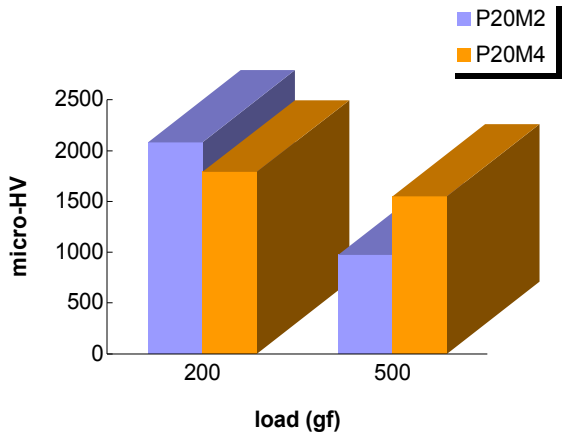

Figure 3.19. Micro-hardness measurements on samples SP20M2 and SP20M4.

For lowest indentation loads, the indents were hardly visible, indicating that, comparing with elastic deformation, the plastic deformation in the diamond films were almost negligible. It has been demonstrated that for a hard film coated in a soft substrate the indentation used to cause a so-called “sink-in” deformation [26 and ref. within]. According to Fan et al. [27], it is viable to assume that for diamond coating on metal substrates under small loads, the deformation of the film is mainly elastic, while the deformation in the substrate is mostly plastic. When the load increases, the contribution of the coating to the composite hardness diminishes and the substrate contribution becomes dominant.
Brinell hardness tests were conducted in a series of samples. An example of the results on composite hardness values are presented in figure 3.20.

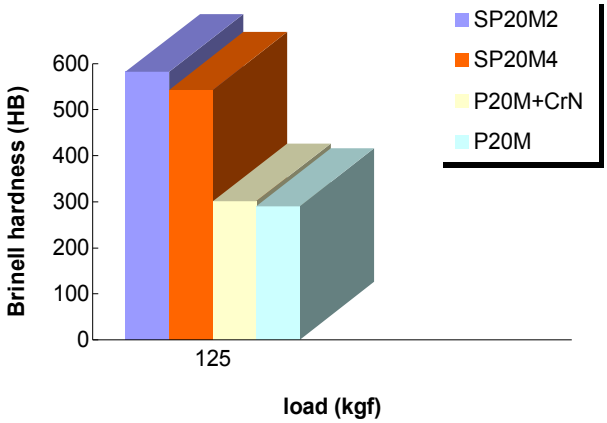

Figure 3.20. Hardness measurements on samples SP20M2, SP20M4, P20M with interlayer and P20M.

The steel ball indentation testing can demonstrate a dependence of the indentation penetration depth on the hardness and thickness of the film [6]. Although having in mind that principle, on figure 3.20 there are shown only the results of hardness obtained for a 125 kgf load, on samples from the original state to the complete coated systems. The variation between SP20M2 and SP20M4 could be related to differences in film thicknesses or deposition time. The values obtained for HB in both samples should have a great contribution from the substrate material.

B) Hardness measurements on AISI 304 samples

Vickers micro-indentation tests were performed in the sample S3048 in a range of loads between 20 gf and 1000 gf. The results on micro-hardness values can be seen in figure 3.21.

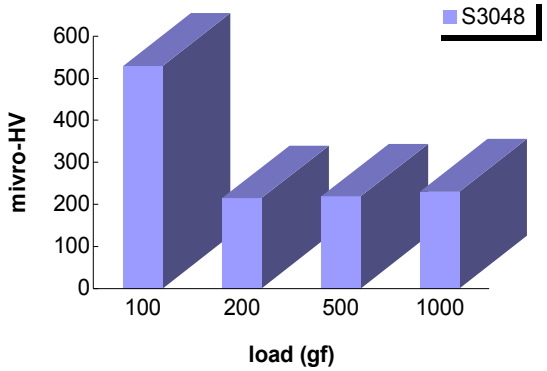

Figure 3.21. Micro-hardness measurements on sample S3048.

For the smaller loads, the indents were hardly visible. The substrate hardness values demonstrate a slight dependence on load for small indentation sizes. This observation is normally associated to the indentation size effect (ISE) phenomenon [32]. The measurements in the coated systems at smaller loads showed improvements in the hardness, demonstrated by its higher values, in comparison to the substrates materials. Coated systems display a considerable increase in hardness with the decrease in the indentation load and consequently the decrease of indentation depth, which could be associated to a less pronounced substrate contribution for the measured values.

Figure 3.21 also demonstrates that, as function of the indentation load at three different areas, when the indentation load increase, the value of hardness decrease and this effect could be observed for all the three selected regions, indicating surface homogeneity. We should not forget that we are testing small areas, trying to make it representative of the entire sample and we should consider the effect of the film thickness variations through the sample. With the increasing of load, the contribution of the coating to the composite hardness lessens at the same time that the substrate contribution becomes dominant.

In figure 3.22, are presented the hardness results obtained on samples S3048, 304 with interlayer and 304 substrate material for a load of 125 kgf.

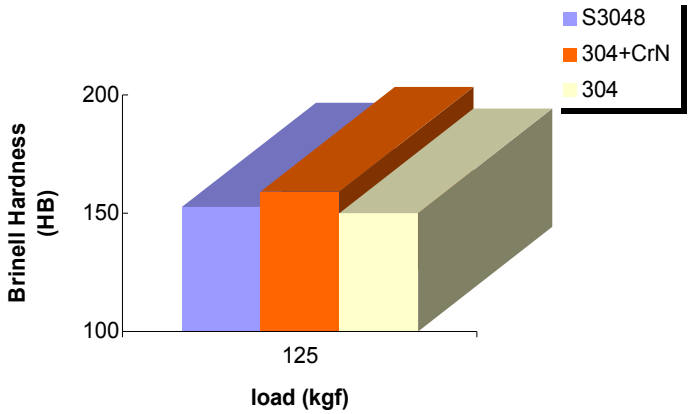

Figure 3.22. Hardness measurements on sample S3048, 304 with interlayer and 304 substrate.

The chart may denunciate that for this load, the diamond film was already delaminated, and in this way, its contribution for the composite system harness is not visible.

References

1. Corrosion Basics-an introduction, National Association of Corrosion Engineers, chapter1 (1984)
2. See f. ex. www.ramada.pt (11.11.2007)
3. See f. ex. http://www.metalravne.com/en (11.11.2007)
4. Stainless Steels, ASM Speciality Handbook, J. R. Davis, Davis &Associates, chapter 1 (1994)
5. See f. ex. webpage *www.prirev.pt* (11.11.2007)
6. J. G. Buijnsters, P. Shankar, W.J.P. van Enckevort, J.J. Schermer and J.J. ter Meulen, "The adhesion of hot-filament CVD diamond films on AISI type 316 austenitic stainless steel", Diamond and Related Materials 13 (2004) 848-857
7. H.S. Nalwa, Handbook of Thin Film Materials, Volume 2: Characterization and Spectroscopy of Thin Films, Chapter 3, (2002) 115- 147
8. C. Bareiβ, M. Perle, S.M. Rosiwal, R.F. Singer, "Diamond coating of steel at high temperatures in hot filament chemical vapour deposition (HFCVD) employing chromium interlayers", Diamond & Related Materials 15 (2006) 754–760
9. Q.H. Fan, E. Pereira and J. Grácio, "Diamond deposition on copper: studies on nucleation, growth, and adhesion behaviours", Journal of Materials Science 34, (1999) 1353 – 1365
10. N.Ali, Q.H.Fan, W.Ahmed and J.Grácio, "Deposition of polycrystalline diamond films using conventional and time modulated CVD processes", Thin Solid Films 420 - 421 (2002) 155 – 160
11. N. Ali, Q.H. Fan, Y. Kousar, W. Ahmed and J. Grácio, "Implementation of the time-modulated process to produce diamond films using microwave-plasma and hot-filament CVD systems", Vacuum 71 (2003) 445 – 450
12. N. Ali , V.F. Neto, Sen Mei, G. Cabral, Y. Kousar, E. Titus, A.A. Ogwu, D.S. Misra and J. Grácio, "Optimisation of the new time-modulated CVD process using the Taguchi method", Thin Solid Films 469–470 (2004) 154–160
13. W. Kulisch, L. Ackermann, B. Sobisch, "On the mechanisms of bias enhanced nucleation of diamond", Physica Status Solidi, A Appl. Res. 154 (1996) 155-174

14. J.W. Ager and M.D. Drory, "Quantitative measurement of residual biaxial stress by Raman spectroscopy in diamond grown on a Ti alloy by chemical vapour deposition", Physical Review B 48 (1993) 2601
15. M.J. Jackson, G.M. Robinson, W. Ahmed, H. Sein, A.N. Jones, N. Ali, E. Titus, Q.H. Fan and J. Grácio, "Time-modulated chemical vapour deposition of diamond films", Journal of Materials Engineering and Performance 14 (2005) 163- 172
16. Q.H. Fan, A. Fernandes, E. Pereira and J. Grácio, "Evaluation of biaxial stress in diamond films", Diamond and Related Materials 8 (1999) 645-650
17. V.G. Ralchenko, A.A. Smolin, V.G. Pereverzev, E.D. Obraztsova et al., "Diamond deposition on steel with CVD tungsten intermediate layer", Diamond and Related Materials 4 (1995) 754-758
18. D. Das, V. Jayaseelan, R. Ramamurti, R.S. Kukreja et al., "Low surface temperature synthesis and characterization of diamond thin films", Diamond and Related Materials 15 (2006) 1336-1349
19. A. Fernandes, A. Neves, R.F. Silva and M.H. Nazaré, "Evaluation of MPCVD diamond film adhesion on hard metal substrates by micro Raman spectroscopy", Diamond and Related Materials 6 (1997) 769-773
20. A. Fayer, O. Glozman, and A. Hoffman, "Deposition of continuous and well adhering diamond films on steel", Applied Physics. Letters 67 16 (1995) 2299-2301
21. R. Polini, G. Mattei, R. Valle and F. Casadei, "Raman spectroscopy characterization of diamond films on steel substrates with titanium carbide arc-plated interlayer", Thin Solid Films 515 (2006) 1011-1016
22. Q.H. Fan, A. Fernandes, E. Pereira and J. Grácio, "Stress-relief behaviour in chemical-vapour-deposited diamond films", Journal of Applied Physics 84 6 (1998) 3155-3158
23. R. Polini, F.P. Mantini, M. Braic et al., "Effects of Ti- and Zr-based interlayer coatings on the hot filament chemical vapour deposition of diamond on high speed steel", Thin Solid Films 494 (2006) 116-122
24. C.F.M. Borges, E. Pfender, J. Heberlein, "Influence of nitrided and carbonitrided interlayers on enhanced nucleation of diamond on stainless steel 304", Diamond and Related Materials 10 (2001) 1983-1990

25. J.C. Bareiβ, G. Hackl, N. Popovska, S.M. Rosiwal, R.F. Singer, “CVD diamond coating of steel on a CVD-TiBN interlayer”, Surface & Coatings Technology 201 (2006) 718–723
26. Q.H. Fan, A. Fernandes, E. Pereira and J. Grácio, “Quantitative evaluation of adhesion of diamond coatings”, Journal of Materials Research 14 3 (1999) 1142-1147
27. Q.H. Fan, A. Fernandes, E. Pereira and J. Grácio, “Adhesion of diamond coatings on steel and copper with a titanium interlayer”, Diamond and Related Materials 8 (1999) 1549-1554
28. N. Ali, G. Cabral, A.B. Lopes and J. Grácio, “Time-modulated CVD on 0.8 μm-WC–10%-Co hardmetals: study on diamond nucleation and coating adhesion”, Diamond and Related Materials 13 (2004) 495–502
29. M.H. Nazaré, A.J. Neves (Eds), “Properties, growth and applications of diamond”, INSPEC, The Institution of Electrical Engineers, London-United Kingdom B2.2 (2001) 303
30. S. Takeuchi, S. Oda, M. Murakawa, “Synthesis of multilayer diamond film and evaluation of its mechanical properties”, Thin Solid Films 398-399 (2001) 238-243
31. N.V. Novikov and S.N. Dub, “Hardness and fracture toughness of CVD diamond film”, Diamond and Related Materials 5 (1996) 1026-1030
32. L. Qian, M.Li, Z. Zhou, H. Yang and X. Shi, “Comparison of nanoindentation hardness to microhardness”, Surface & Coatings Technology 195 (2005) 264-271

Chapter 4.

Conclusions and proposals for future work

The exceptional potential of CVD diamond coatings for technical applications, allowing the improvement on mechanical components performance and increasing tools life time, justifies the importance of this study.

Steels are of special interest, because of the widely use on the manufacture of engineering components. The deposition of a well adherent diamond coating on a steel component, could have an enormous advantage for very demanding applications. Nevertheless, deposition of diamond CVD on steel still presents some difficulties due the nature of substrate and coating.

This dissertation intends to contribute to the evolution on scientific knowledge on this field, reporting a study on diamond growth on different steel substrates: AISI 304, 310, 316 and P20 modified. Diamond films were deposited using a time-modulated CVD (TMCVD) process. A CrN interlayer was deposited on the samples, before diamond deposition.

The effectiveness of the CrN interlayer was considered. EDS from the interlayer surface deposited on steel samples, shown good results in terms of barrier diffusion of elements from the substrate materials. X-ray mapping of samples cross section confirmed the above data.

Different deposition cycles were investigated in order to achieve the best meeting for diamond films growth. There were two separated components on the research work and the investigation results were divided in four separated studies. On one hand, was presented a comparison on the results obtained for samples of diamond P20 mod. steel samples, after two different deposition conditions. On the other hand, were presented the results from a diamond coated 304 steel sample.

The study 1, correspond to the diamond growth using different TMCVD conditions. The variations in nucleation density and morphology were observed, as well as the effect of CH_4/H_2 flow rate modulations and temperature variations, for the different TMCVD cycles. After the first studies on AISI 310 and 316 steel samples, that presented the weaker results in terms of diamond nucleation, for the experimental conditions in use, those

materials were abandoned for this investigation. A possible explanation for the results can be related with some chemical composition effect of these materials. Samples of AISI P20 modified and AISI 304 steels, were successfully coated with diamond.

The study 2, consisted on an evaluation of the residual stresses developed in samples with continuous diamond films, from P20mod. and AISI 304 steels. The films were examined and characterized by SEM, EDS, Raman spectroscopy and indentation tests.

The compression residual stresses present on samples demonstrate to depend essentially on the characteristics of the substrate material, mainly on terms of thermal expansion coefficient. Samples of P20mod. showed a value of thermal stress of -9.78 GPa, whereas samples of 304 steel presented a value of -12.82 GPa.

In study 3, was made an estimation of film adhesion on samples of the two steels, using indentation techniques. After indentation at small loads, the Raman spectrums shifted to lower wavernumbers, closer to 1332 cm^{-1}. This feature demonstrate a stress relieve of the films after indentation at small loads. Brinell indentations demonstrated that the film delamination starts on P20mod. samples, at indentation loads of 125 kgf. On 304 steel samples the film seemed to begin to delaminate between 20 kgf and 50 kgf applied loads.

Study 4, present an evaluation of the hardness profiles in different stages of the process of study. The influence of the substrate hardness on the composite system harness and the hardness variation after diamond deposition was identified in all the cases.

From the global results, it is possible to affirm, that diamond deposition on those steel substrates, using TMCVD processes showed promising results for technological applications. However, for future work, it would be necessary to complement the present study with complementary morphological and mechanical testing, in order to guarantee the reproducibility of the results.

The evaluation of surface roughness, wear resistance and friction coefficient will be of great importance to consider for technological application development.